chromosome 3 clone RP11-61K12 (AC011199). We synthesized gene-specific primers and genotyped each individuals by PCR-SSCP analysis. The genotype frequency of the 82133G>A polymorphism of human chromosome 3 clone RP11-61K12 (AC011199) differed significantly (P= 0.0189, Fisher's exact test) between older subjects (>90 years) and younger subjects (<70 years) (Table 2). Differences in allele and genotype frequencies between the four age categories were not statistically significant.

The SNP was located in a mammalian-wide interspersed repeat (MIR) on chromosome 3 and was described in GeneBank. MIRs are one of the most common interspersed repeats in primates, with an estimated 300,000 copies per genome that account for 1–2% of the total DNA [6]. It is not clear whether this SNP is associated with longevity; however, it is noteworthy that the strategy we describe herein was useful for identifying an SNP that showed statistically significant differences in its distribution across the subject groups.

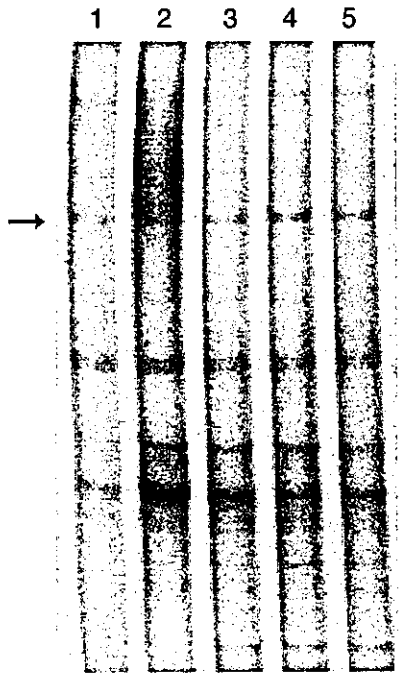

Fig. 1. Electropherogram of AP-PCR-SSCP. The AP-PCR product amplified by using Ae6R primer was separated by SSCP analysis (6% polyacrylamide gel electrophoresis at 15 °C for 5 h). A stained band with different mobility and density (shown as arrow; observed as slightly broad band in lane 1) was excised from the gel, cloned, and sequenced. As a result of sequential examinations, an SNP of the human chromosome 3 clone was found. Lane 1, individuals aged more than 100 years (n=9); lanes 2–4, individuals aged 90–99 years (3 sub-groups, n=8 each group); lane 5, individuals aged 60–69 years (n=9).

Table 2
Genotype and allele frequencies of the 82133G>A polymorphism on human chromosome 3 clone RP11-61K12 (AC011199) in subjects classified by age

Age	Genotype			G allele		A allele	
	G/G	G/A	A/A	No.	%	No.	%
≥100 years	4	5	0	13	72	5	28
90–99 years	10	11	0	31	74	11	26
60–69 years	1	6	2	8	44	10	56
<30 years	9	13	5	31	57	23	43
>90 years	13*	16*	0*	44	73	16	27
<70 years	10*	19*	7*	39	54	33	46

* The genotype frequency differed significantly (P=0.0189, Fisher's exact test) between older subjects (>90 years) and younger subjects (<70 years).

In the present pilot study, we used mini-gel, for SSCP. If large gels with long separations or 2-dimensional separation with detection by fluorescence dyes are used, better resolution could be obtained. Both the phenotype-to-genotype screening strategy and semi-quantitative distribution measurement using pooled DNA may be useful in screening for important genetic variations associated with a variety of human diseases and phenotypes. The advanced improvement of precise techniques is clearly necessary, however, the pooled DNA strategy and quantitative genotype discrimination can also indicate the relative proportion of different genotypes, haplotypes or allelotypes at glance and be applied to screening for the relationship between phenotype and genotype more effectively.

Acknowledgements

This research was supported in part by Health and Labor Sciences Research Grants for Third Term Comprehensive Control Research for Cancer (H15-9 and H16-018), by Grants-in-Aid for Exploratory Research (15659133) from the Japan Society for the Promotion of Science, and by the Nakatani Electronic Measuring Technology Association of Japan.

References

[1] Um J-Y, Lee K-M, Kim H-M. Polymorphism of interleukin-1 receptor antagonist gene and obesity. Clin Chim Acta 2004; 340:173–7.

[2] Welsh J, McClelland M. Fingerprinting genomes using PCR with arbitrary primers. Nucleic Acids Res 1990;18:7213–8.

[3] Peinado MA, Malkhosyan S, Velazquez A, Perucho M. Isolation and characterization of allelic losses and gains in colorectal tumors by arbitrarily primed polymerase chain reaction. Proc Natl Acad Sci U S A 1992;89:10065–9.

[4] Maekawa M, Sugano K, Ushiama M, Masuda T, Ohkura H, Kakizoe T, et al. Relative ratios of mRNA molecules encoded by genes with homologous sequences using fluorescence-based single-strand conformation polymorphism analysis. Biochem Biophys Res Commun 1996;223:520–5.

[5] National Center for Biotechnology Information. BLAST. http://www.ncbi.nlm.nih.gov/BLAST/.

[6] Smit AF, Riggs AD. MIRs are classic, tRNA-derived SINEs that amplified before the mammalian radiation. Nucleic Acids Res 1995;23:98–102.

Problem with Detection of an Insertion-Type Mutation in the *BCHE* Gene in a Patient with Butyrylcholinesterase Deficiency, *Masato Maekawa,*[1*] *Terumi Taniguchi,*[1] *Jinko Ishikawa,*[1] *Shigeru Toyoda,*[2] *and Noriko Takahata*[2] ([1] Department of Laboratory Medicine, Hamamatsu University School of Medicine, Hamamatsu, Japan; [2] Department of Pediatrics, Hospital affiliated with Kanagawa Prefecture School of Nursing and Midwifery, Yokohama, Japan; * address correspondence to this author at: Department of Laboratory Medicine, Hamamatsu University School of Medicine, Hamamatsu 431-3192, Japan; fax 81-53-435-2794, e-mail mmaekawa@hama-med.ac.jp)

Genetic variants of human butyrylcholinesterase (EC 3.1.1.8; serum cholinesterase; pseudocholinesterase; BCHE) are reported to be associated with prolonged apnea in patients taking the muscle relaxant drug succinylcholine *(1)* and with low serum BCHE activity *(2)*. The gene encoding BCHE is at least 73 kb long and contains one noncoding and three coding exons *(3)*. Genetic variants of *BCHE* have been reported *(2, 4–8)*. We analyzed *BCHE* mutations in the Japanese population *(2, 4–6)*. The *BCHE* mutations found in study populations in the United States have been quite different from those found in Japanese study populations *(2, 7)*. An atypical variant of BCHE has been detected in Caucasians but not in Japanese populations, but fluoride-resistant genes have been reported in Japanese populations as well as Caucasian populations *(5, 6)*.

We recently detected an abnormal genotype in members of a family with low serum BCHE activity. This family carried an insertion mutation in the *BCHE* gene. Although PCR techniques are now used routinely in genetic testing, there are still possible sources of errors that researchers must be aware of and consider when designing assays. In this report, we present an important example of a pitfall in mutation detection.

Routine laboratory examination identified very low serum BCHE activity (42 U/L) in a 1-year-old boy (reference interval, 4250–7250 U/L). Because secondary hypocholinesterasemia attributable to hepatic dysfunction or organophosphorus poisoning was ruled out on the basis of other biochemical data and clinical symptoms, the child was thought to be homozygous for a silent *BCHE* gene. The serum BCHE activities in his mother and father were 3009 and 3767 U/L, respectively. Serum BCHE activity was measured spectrophotometrically with butyrylthiocholine iodide (EIKEN CHEMICAL) as a substrate at 37 °C on a JCA-BM2250 automated biochemistry analyzer (JEOL). Genetic analysis was performed after approval from the Institutional Review Board of Hamamatsu University School of Medicine, and informed consent was obtained from all family members.

Genomic DNA was extracted from EDTA-treated venous blood as described by Kunkel et al. *(9)*. Coding exons of the *BCHE* gene were amplified as nine independent fragments by PCR, and each amplified product was analyzed by single-stranded DNA conformation polymorphism analysis *(2, 4)* and denaturing HPLC (WAVE System; Transgenomic). PCR products with variant migration patterns were sequenced directly with a BigDye Terminator Cycle Sequencing FS Ready Reaction Kit and a PRISM 310 Genetic Analyzer (Applied Biosystems). Bands with different mobilities were excised from the gel and cloned into pDRIVE (Qiagen) for sequencing. The mutation was confirmed by PCR-restriction fragment length polymorphism analysis.

We detected a G-to-C missense mutation at codon 365 (G365R) in exon 2 of *BCHE*. The proband was homozygous for this mutation, his father was heterozygous, and his mother was homozygous wild type. Representative DHPLC and sequencing results are shown in panels A and B of supplemental Fig. 1, which appears in the Data Supplement that accompanies the online version of this Technical Brief at http://www.clinchem.org/content/vol50/issue12/. We confirmed our results with PCR-restriction fragment length polymorphism analysis using *TaqI* (Fig. 2 in the online Data Supplement). If our results are correct, the pedigree and genotype segregations are not easily understood. Hemizygosity of the region containing the G365R site resulting from a large deletion, an inversion, uniparental disomy (genomic imprinting), or a de novo mutation may explain the pedigree. We first tried long PCR to address the possibility of a large deletion, but the result did not provide a clear explanation for the pedigree. We did, however, notice a faint band that migrated more slowly than the target PCR product for exon 2. We therefore changed the extension time of the amplification conditions. The results obtained by electrophoresis on an agarose gel of PCR products from reactions performed with different extension time is shown in Fig. 1. When longer extension times were used, PCR product was longer. We suspected an insertion mutation and therefore excised the longer fragment from the gel and subcloned and sequenced it. We identified an abnormal sequence inserted in exon 2 as an *Alu* sequence and a direct repeat (300 + 15 bp). This inserted sequence may have caused premature termination of transcription (Fig. 3 in the online Data Supplement). Both the proband and his mother were heterozygous for this insertion. We therefore concluded that the proband was a compound heterozygote for the G365R missense mutation and the *Alu* insertion mutation.

Alu sequences are short interspersed elements that are distributed widely throughout the human genome *(10)*. *Alu* sequences can be divided into subfamilies of related

	Temperature	Routine protocol (min)	Trial protocol (min)	Cycle
Pre-denaturation	94	3	3	1
Denaturation	94	0.5	0.5	30
Annealing	57	0.5	0.5	
Extension	72	0.6	x	
Post-extension	72	5	5	1

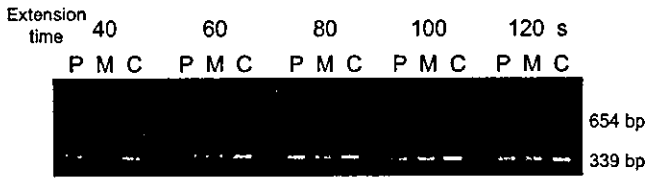

Fig. 1. Agarose gel electrophoresis of the PCR products amplified with different extension times.

PCR reactions were performed in 25 μL containing 50 ng of DNA, 100 μM each deoxynucleotide triphosphate, 1.5 mM $MgCl_2$, 12.5 pmol of each primer, 0.75 U of AmpliTaq Gold DNA polymerase, and 1× Gold Buffer (Applied Biosystems) on a GeneAmp PCR System 9700 (Applied Biosystems). (*Top*), PCR conditions. Extension time varied from 40 to 120 s at 20-s intervals. (*Bottom*), PCR products separated by electrophoresis on a 2% agarose gel. *P*, proband; *M*, mother; *C*, wild-type control. Extension time is indicated *above* each sample group.

elements on the basis of diagnostic mutations that are shared by subfamily members. The family described here is the second reported in which insertion of an *Alu* has caused BCHE deficiency; the first was described by Muratani et al. *(8)*. Although the *Alu* sequence in the present study was classified as *Alu*Yb8 because of similarities with the *Alu*Yb8 reported by Muratani et al. *(8)*, it also differed at several nucleotides.

In the present study, if genetic analysis had been performed only on the proband, he would have been misdiagnosed as homozygous for the G365R mutation. Analysis of the family revealed a discrepancy in genotype segregation, which directed us to additional analyses and allowed us to reach the proper conclusion. Shorter PCR programs are convenient for mutation detection, but fragments that are longer than expected may not be amplified and would therefore be missed. We conclude from our present experience that PCR with short extension times may be a source of pitfalls in mutation detection.

References

1. Kalow W, Genest K. A method for the detection of atypical forms of human serum cholinesterase; determination of dibucaine numbers. Can J Med Sci 1957;35:339–46.
2. Maekawa M, Sudo K, Dey DC, Ishikawa J, Izumi M, Kotani K, et al. Genetic mutations of butyrylcholine esterase identified from phenotypic abnormalities in Japan. Clin Chem 1997;43:924–9.
3. Arpagaus M, Kott M, Vatsis KP, Bartels CF, La Du BN, Lockridge O. Structure of the gene for human butyrylcholinesterase. Evidence for a single copy. Biochemistry 1990;29:124–31.
4. Maekawa M, Sudo K, Kanno T, Kotani K, Dey DC, Ishikawa J, et al. Genetic basis of the silent phenotype of serum butyrylcholinesterase in three compound heterozygotes. Clin Chim Acta 1995;235:41–57.
5. Dey DC, Maekawa M, Sudo K, Kanno T. Butyrylcholinesterase genes in individuals with abnormal inhibition numbers and with trace activity: one common mutation and two novel silent genes. Ann Clin Biochem 1998;35:302–10.
6. Sudo K, Maekawa M, Akizuki S, Magara T, Ogasawara H, Tanaka T. Human butyrylcholinesterase L330I mutation belongs to a fluoride-resistant gene, by expression in human fetal kidney cells. Biochem Biophys Res Commun 1997;240:372–5.
7. Primo-Parmo SL, Bartels CF, Wiersema B, van der Spek AF, Innis JW, La Du BN. Characterization of 12 silent alleles of the human butyrylcholinesterase (BCHE) gene. Am J Hum Genet 1996;58:52–64.
8. Muratani K, Hada T, Yamamoto Y, Kaneko T, Shigeto Y, Ohue T, et al. Inactivation of the cholinesterase gene by *Alu* insertion: possible mechanism for human gene transposition. Proc Natl Acad Sci U S A 1991;88:11315–9.
9. Kunkel LM, Smith KD, Boyer SH, Borgaonkar DS, Wachtel SS, Miller OJ, et al. Analysis of human Y-chromosome-specific reiterated DNA in chromosome variants. Proc Natl Acad Sci U S A 1977;74:1245–9.
10. Deininger PL, Batzer MA. *Alu* repeats and human disease. Mol Genet Metab 1999;67:183–93.

DOI: 10.1373/clinchem.2004.041129

Carcinogenesis vol.25 no.12 pp.2311–2317, 2004
doi:10.1093/carcin/bgh267

Inactivating mutations of the human base excision repair gene *NEIL1* in gastric cancer

Kazuya Shinmura[1], Hong Tao[1], Masanori Goto[1], Hisaki Igarashi[1], Terumi Taniguchi[2], Masato Maekawa[2], Toshiro Takezaki[3] and Haruhiko Sugimura[1,4]

[1]First Department of Pathology and [2]Department of Laboratory Medicine, Hamamatsu University School of Medicine, 1-20-1 Handayama, Hamamatsu, Shizuoka 431-3192, Japan and [3]Department of International Island and Community Medicine, Kagoshima University Graduate School of Medical and Dental Sciences, 8-35-1 Sakuragaoka, Kagoshima 890-8544, Japan

[4]To whom correspondence should be addressed
Email: hsugimur@hama-med.ac.jp

Oxidized DNA base lesions, such as thymine glycol (Tg) and 8-hydroxyguanine, are often toxic and mutagenic and have been implicated in carcinogenesis. To clarify whether NEIL1 protein, which exhibits excision repair activity towards such base lesions, is involved in gastric carcinogenesis, we examined 71 primary gastric cancers from Japanese patients and four gastric cancer cell lines for mutations and genetic polymorphisms of the *NEIL1* gene. We also examined 20 blood samples from Chinese patients for *NEIL1* genetic polymorphisms. Three mutations (c.82_84delGAG:p.Glu28del, c.936G>A and c.1000A>G:p.Arg334Gly) and two genetic polymorphisms were identified. When the excision repair activity towards double-stranded oligonucleotide containing a Tg:A base pair was compared among six types of recombinant NEIL1 proteins, p.Glu28del-type NEIL1, found in a primary case, was found to exhibit an extremely low activity level. Moreover, c.936G>A, located in the last nucleotide of exon 10 and detected in the KATO-III cell line, was shown to be associated with a splicing abnormality using an *in vivo* splicing assay. An immunofluorescence analysis showed that the wild-type NEIL1 protein, but not the truncated protein encoded by the abnormal transcript arising from the c.936G>A mutation, was localized in the nucleus, suggesting that the truncated protein is unlikely to be capable of repairing nuclear DNA. An expression analysis revealed that NEIL1 mRNA expression was reduced in six of 13 (46%) primary gastric cancer specimens that were examined. These results suggest that low NEIL1 activities arising from mutations and reduced expression may be involved in the pathogenesis in a subset of gastric cancers.

Introduction

Oxidative DNA damage is widely accepted to be a causative factor of cancer; this type of damage includes pre-mutagenic and blocking lesions that may lead to mutation and cell death, respectively (1,2). 8-Hydroxyguanine (oh8G) and thymine glycol (Tg) are typical examples of the former and latter lesions, respectively, and are used as biomarkers of oxidative stress (1–3). The base excision repair pathway is a universal mechanism for such base lesions in DNA and is initiated by DNA glycosylases that hydrolyze the *N*-glycosidic bond, releasing the damaged base from double-stranded DNA. Human DNA glycosylases encoded by the *OGG1* (MIM# 601982) and *NTH1* (MIM# 602656) genes have the activity to remove oh8G and Tg from DNA, respectively (4–12). So far, *OGG1* somatic mutations have been reported in some types of cancers, and the impairment of DNA repair activity in these mutant proteins has been proven experimentally (13–16). In these papers, the impaired DNA repair activity of the OGG1 protein was speculated to lead to an accumulation of oxidative DNA damage and an increase in the mutation rate of cells, which may be related to cancer. Moreover, an association between the *OGG1* genetic polymorphism and cancer has also been reported (17,18). The *NEIL1* gene (MIM# undecided) has been isolated recently and revealed to encode DNA glycosylase for oh8G and Tg (19–26). Judging from the similarity of the substrates, an investigation of the somatic mutations and genetic polymorphisms of the *NEIL1* gene would seem to be worthwhile. Stomach tissue, in particular, is exposed to oxidative stresses, including inflammation induced by sodium chloride, *Helicobacter pylori* infection and smoking (27–29). The huge amounts of oxidative DNA damage may play an important role in carcinogenesis and a predisposition to gastric cancer. Therefore, in this study, we examined primary gastric cancers for somatic mutations and genetic polymorphisms of the *NEIL1* gene and assessed the functional status of the detected *NEIL1* variants. We also assessed NEIL1 expression in tumor tissue. This is the first report to describe a genetic alteration of the *NEIL1* gene in human cancer tissue.

Abbreviations: FITC, fluorescein 5-iso-thiocyanate; oh8G, 8-hydroxyguanine; PAGE, polyacrylamide gel electrophoresis; PBGD, porphobilinogen deaminase; PCR, polymerase chain reaction; QRT-PCR, quantitative real-time-PCR; RT-PCR, reverse transcription-PCR; Tg, thymine glycol

Materials and methods

Samples

Gastric cancers from a total of 71 sporadic cases and corresponding normal mucosae were obtained from Hamamatsu University Hospital, Shizuoka, Japan. The four gastric cancer cell lines used in this study were MKN45, MKN74, TMK-1 and KATO-III (30). Blood samples from a total of 20 Chinese primary gastric cancer patients were obtained from Huaian City Municipal Hospital, China (31). The protocol was approved by the Human Institutional Review Board of Hamamatsu University School of Medicine. DNA was extracted by standard SDS-proteinase K digestion followed by phenol-chloroform extraction and ethanol precipitation.

NEIL1 variant screening

NEIL1 variants were screened with the WAVE DNA Fragment Analysis System (Transgenomic, Omaha, NE). The method is based on ion-pair, reverse-phase high-performance liquid chromatography and temperature-modulated heteroduplex analysis. Nine coding exons of the *NEIL1* gene were amplified by genomic polymerase chain reaction (PCR) using 10 sets of primers: 5′-AGC CGC TAC CTC ACA AAG TC-3′ and 5′-GCT GAA AAG

AGC CGG ACA TG-3′ for exon 4a, 5′-CTA CCG CAT CTC AGC TTC AG-3′ and 5′-AGA AGG CAC TAA GAG AGT CAG-3′ for exon 4b, 5′-ACG CAC CCA GAC CGT GTT C-3′ and 5′-GGC AAG CCA TGC TAG GCA G-3′ for exon 5, 5′-AGA GAT CCT GTA CCG GTC AG-3′ and 5′-CCC CTG TTG TTG AGC TAA GC-3′ for exon 6, 5′-AGC TCA GAG AGA AGG TCA GC-3′ and 5′-TGC TGA AGC AGA GGT TGC TG-3′ for exon 7, 5′-TCA GTC CAT CAG CTT GTG TAG-3′ and 5′-CTA GAC AGA CCC TGA GCA TC-3′ for exon 8, 5′-CCT GCC TCT CCA AGG AAT AC-3′ and 5′-TGT AGC CCT TGC AGG CGT G-3′ for exon 9, 5′-CCA ACT CCA ACA CCA GTG TC-3′ and 5′-AGG GTA AGG CAG CTG CCT G-3′ for exon 10, 5′-ACC TCT GAA CTG CTT TCT GAG-3′ and 5′-CTT TGT ACA CGC GCT CCT AG-3′ for exon 11, and 5′-CAG CCC CTG GAG TCT TAG C-3′ and 5′-ACC TTC AGA TAT TGC CTG CTC-3′ for exon 12. PCR was performed in 25 μl reaction mixtures containing AmpliTaq Gold (Applied Biosystems, Tokyo, Japan) under the following conditions: 30 s at 94°C, 30 s at 56°C and 60 s at 72°C for 35 cycles. PCR products were analyzed using WAVE and WAVEMaker software 4.0 (Transgenomic). PCR products exhibiting different peaks in the WAVE analysis were directly sequenced using a BigDye Terminator Cycle Sequencing Reaction Kit and the ABI 3100 Genetic Analyzer (Applied Biosystems).

Preparation of the recombinant NEIL1 proteins

NEIL1 protein tagged with His_6 at its C-terminus was prepared according to the pET System protocol (Novagen, Darmstadt, Germany). Briefly, *NEIL1* cDNA-containing pET25b(+) vector was constructed by inserting a PCR product of NEIL1 cDNA into the *Nde*I and *Xho*I sites of a pET25b(+) vector (Novagen). *Escherichia coli* BL21-CodonPlus (DE3)-RP competent cells (Stratagene, La Jolla, CA) were transformed with the *NEIL1* cDNA-containing pET25b vectors and cultured at 37°C until A_{600} reached 0.5. After incubation with 0.5 mM isopropyl-1-thio-β-D-galactopyranoside (IPTG) at 25°C for 12 h, NEIL1-His_6 protein was purified using TALON metal affinity resins (Clontech, Palo Alto, CA) under native conditions according to the manufacturer's instructions. The protein was then dialyzed against the buffer containing 20 mM sodium phosphate (pH 7.5), 50 mM NaCl, 1 mM dithiothreitol, 1 mM EDTA, 1 mM phenylmethylsulfonylfluoride and 20% glycerol. The quality and concentration of the protein were determined using an Agilent 2100 Bioanalyzer (Agilent Technologies, Palo Alto, CA). For the construction of the vector for the NEIL1variant forms, a QuikChange Site-Directed Mutagenesis kit (Stratagene) was used.

DNA cleavage activity assay

A 30mer oligonucleotide containing or not containing a single 5*R*,6*S*-Tg (5′-CTG GTG GCC TGA C[Tg or T]C ATT CCC CAA CTA GTG-3′) was chemically synthesized and purified by polyacrylamide gel electrophoresis (PAGE) (Japan Bio Services, Saitama, Japan). The oligonucleotide was ^{32}P-labeled at the 5′ terminus with a MEGALABEL kit (Takara, Osaka, Japan) and [γ-^{32}P]ATP (Amersham Biosciences, Piscataway, NJ) and annealed to a complementary strand containing an adenine opposite the Tg or T. The reaction was performed with 20 μl of a mixture containing 25 nM NEIL1-His_6 protein, 20 mM sodium phosphate (pH 7.5), 50 mM NaCl, 1 mM dithiothreitol, 1 mM EDTA, 2.5 nM labeled DNA and 50 μg/ml bovine serum albumin at 37°C. After the reaction, denaturing formamide dye was added to the mixture, heated at 95°C for 3 min, and subjected to 20% PAGE. A 13mer oligonucleotide (5′-CTGGTGGCCTGAC$_P$-3′) was ^{32}P-labeled at the 5′ terminus and used as a size marker for the cleaved products. The radioactivities of intact and cleaved oligonucleotides were quantified using a bioimaging analyzer (BAS1000, Fuji Photo Film, Tokyo) and ImageGauge software (Fuji Photo Film).

RNA isolation and reverse transcription (RT)–PCR

Total RNA was extracted with an RNeasy Mini Kit (Qiagen, Valencia, CA) and converted to first-strand cDNA with a SuperScript First-Strand Synthesis System for RT–PCR (Invitrogen, Carlsbad, CA) according to supplier's protocol. PCR amplification was performed using the following sets of primers: 5′-GAA ATC CAA GGC CAC ACA GC-3′ and 5′-TTG CAG TCC TCT TAG GAA GGT C-3′ for NEIL1 transcripts and 5′-CCA AGG TCA TCC ATG ACA AC-3′ and 5′-CAC CCT GTT GCT GTA GCC A-3′ for GAPDH transcripts. PCR products were fractionated by electrophoresis on an agarose gel and stained with ethidium bromide. The band detected by electrophoresis was excised from the gel and directly sequenced.

In vivo splicing assay

NEIL1-936G and -936A type vectors were constructed by inserting a PCR product of the *NEIL1* gene into the *Eco*RI and *Mlu*I sites of a pALTER-MAX (Promega, Madison, WI) mammalian expression vector, as indicated in Figure 2C. The expression vectors were transfected into a lung cancer cell line, NCI-H1299, using the LipofectAMINE 2000 reagent (Invitrogen) according to the supplier's recommendations. At 24 h post-transfection, the cells were harvested, and total RNA was extracted and converted to cDNA. RT–PCR was performed using a set of primers, pAM-F (5′-CAG CTC TTA AGG CTA GAG TAC-3′) and pAM-R (5′-CTT ATC ATG TCT GCT CGA AGC-3′), and PCR products were fractionated by agarose gel electrophoresis.

Immunofluorescence analysis

Wild-type and truncated-type NEIL1 expression vectors containing a FLAG tag were constructed by inserting each cDNA with the FLAG sequence at the C-terminus into the *Xba*I and *Eco*RI sites of a pcDNA3.1(+) plasmid vector (Invitrogen). The p.Arg334Gly type NEIL1 expression vector was prepared using a QuikChange Site-Directed Mutagenesis kit (Stratagene) and a wild-type NEIL1-FLAG expression vector. The expression vector was then transfected into NCI-H1299 cells using LipofectAMINE 2000 reagent (Invitrogen), according to the supplier's recommendations. After 24 h, the cells were fixed with 4% paraformaldehyde. After microwave treatment and permeabilization, the cells were incubated with 40 μg/ml of anti-FLAG M2 antibody (Sigma, St Louis, MO) at room temperature for 1 h. Indirect immunofluorescence labeling was performed using a fluorescein 5-iso-thiocyanate (FITC)-conjugated anti-mouse IgG secondary antibody (Cappel, Aurora, OH) at room temperature for 30 min, and the nuclei were stained with 4′-6-diamidino-2-phenylindole (DAPI) (Vysis, Downers Grove, IL). The slides were examined under a fluorescence microscope (Olympus BX-50-FL; Olympus) equipped with epi-fluorescence filters and a photometric CCD camera (Quantix 1400; Roper Scientific, Tucson, AZ). The images captured were digitized and stored in the image analysis program (IPlab Spectrum; Scanalytics, Fairfax, VA).

Quantitative real-time (QRT)–PCR

Expression of the NEIL1 mRNA transcript was measured by QRT–PCR using a LightCycler instrument (Roche, Palo Alto, CA). The specimens available for analysis of its expression represented only a small fraction (18.3%: 13 of 71 cases) of the surgical specimens, because (i) most of the surgical specimens were small; (ii) nothing was left after most of the surgical specimens had been used for DNA extraction; and (iii) RNA samples of clearly low quality were rejected. The mirror section of the tissue sample for RNA extraction was confirmed to have the proper components using hematoxylin and eosin staining. PCR amplification of the NEIL1 transcript and the transcript of a control housekeeping gene, *porphobilinogen deaminase* (*PBGD*), was performed using a QuantiTect SYBR Green PCR kit (Qiagen). The following PCR primers were used: 5′-AGA AGA TAA GGA CCA AGC TGC-3′ and 5′-GAT CCC CCT GGA ACC AGA TG-3′ for the NEIL1 transcript and 5′-GTC TGG TAA CGG CAA TGC GG-3′ and 5′-TCC CCT GTG GTG GAC ATA GC-3′ for the PBGD transcript. The relative amounts of NEIL1 transcript were standardized according to those of the PBGD transcript. The relative expression of each sample was calculated by comparing the expression of non-cancerous gastric tissue in a primary gastric cancer patient (case no. 1). The T/N ratio was calculated in each case.

Statistics

A Wilcoxon signed-ranks test was performed using StatView software (Abacus Concepts, Berkeley, CA).

Results

Identification of NEIL1 mutations in gastric cancer

We examined 71 primary gastric cancers from Japanese patients and four gastric cancer cell lines for mutations and genetic polymorphisms of the *NEIL1* gene. We also examined blood samples from 20 Chinese primary gastric cancer patients for genetic polymorphisms of the *NEIL1* gene. A survey for all the coding sequences of the *NEIL1* gene with intronic or non-coding sequence-based primers disclosed three mutations (c.82_84delGAG:p.Glu28del, c.936G>A and c.1000A>G: p.Arg334Gly) and two genetic polymorphisms (Table I). None of the three mutations were observed in any of the non-cancerous tissues examined in this study, and all of the mutations were observed in heterozygosity.

Impairment in Tg DNA glycosylase activity of mutant-type NEIL1 protein

To assess the functional status of the proteins coded by the variant-type *NEIL1* genes, each type of recombinant NEIL1 protein tagged with His_6 at its C-terminus was prepared by site-directed mutagenesis in a wild-type *NEIL1*

Table I. Somatic mutations and genetic polymorphisms of the *NEIL1* gene

Exon/intron[a]	Nucleotide change[b]	Predicted effect (polypeptide length[c])	Sample	Allele frequency[d]	
				Japanese	Chinese
Somatic mutation					
Exon 4	c.82_84delGAG	p.Glu28del (389 aa)	GC-16 (surgical specimen)	0.000	0.000
Exon 10	c.936G>A	splicing abnormality (337 aa)	KATO-III (cell line)	0.000	0.000
Exon 11	c.1000A>G	p.Arg334Gly (390 aa)	GC-71 (surgical specimen)	0.000	0.000
Genetic polymorphism					
Intron 7	[c.719-80delT + c.719-82T>G]	Unknown	JS-159 (blood sample)	0.000	0.025
Exon 8	c.733G>A	p.Gly245Arg (390 aa)	JS-158 (blood sample)	0.000	0.025

[a]According to LocusLink homepage (Locus ID: 79661) of the NCBI web site.
[b]Nucleotide +1 is the A of the ATG-translation initiation codon.
[c]Length of wild-type NEIL1 protein: 390 aa.
[d]The allele frequencies were determined using analyses of non-cancerous tissues from Japanese and Chinese patients with gastric cancer.

cDNA-containing pET25b(+) expression vector. Since the N-terminal Pro2 is an active site (19), we also prepared a p.Pro2del construct as a negative control. Although a p.Lys242Arg variant was not detected in the present series, this variant and p.Lys245Arg variant described here is available on the LocusLink homepage of the NCBI Web Site. Thus, we also prepared a p.Lys242Arg construct. In total, six recombinant NEIL1-His_6 proteins, including a wild-type protein, were expressed in *E.coli* and purified to apparent homogeneity (Figure 1A). Their molecular size of ~47 kDa was determined by SDS-PAGE and corresponded with that calculated from the cDNA sequences. The Tg DNA glycosylase activity of the NEIL1 protein was tested by determining its capacity to cleave a double-stranded oligonucleotide containing a Tg:A mispair (Figure 1B and C). The enzymatic activities of the p.Lys242Arg, p.Gly245Arg and p.Arg334Gly type proteins were similar to that of the wild-type protein. However, the enzymatic activity of the p.Glu28del type protein was similar to that of the p.Pro2del type protein, indicating a strong impairment in the DNA repair activity of the p.Glu28del type protein.

Effect of the NEIL1 c.936G>A mutation on pre-mRNA splicing and subcellular localization

c.936G>A was detected in one gastric cancer cell line, KATO-III. As this nucleotide substitution has not been found in any other samples, it is probably a somatic mutation. However, as DNA from corresponding normal tissue for the KATO-III cell line was not available, we could not exclude the possibility that this substitution might be a rare genetic polymorphism. c.936G>A was located in the last nucleotide of exon 10. Guanine at the last nucleotide of the exon resides in the consensus sequence at the 5′ splice site, which is recognized and bound by U1 small nuclear RNP during 5′ splice site selection (32). Moreover, the G>A change at the last nucleotide of the exon in the *OGG1* gene was associated with the retention of the following intron (13). Therefore, the c.936G>A change in the *NEIL1* gene may weaken the splicing signal. RT-PCR and sequencing analyses revealed that a NEIL1 mRNA transcript derived from KATO-III cells, but not from TMK-1 cells, contained a 160-bp intron 10 sequence (Figure 2A, band II). The transcript derived from KATO-III cells encoded the truncated-type NEIL1 protein (Figure 2B). To confirm the contribution of c.936G>A to this splicing abnormality, a pALTER-MAX mammalian expression vector was inserted by a PCR product containing c.936G or c.936A and surrounding the *NEIL1* sequence, including intron 10, as illustrated in Figure 2C. These vectors and parental pALTER-MAX vector were then transfected into NCI-H1299 cells, and the total RNA was extracted from these cells. An RT-PCR analysis using a set of primers for the pALTER-MAX sequence and a sequencing analysis of the bands on the gel revealed that a transcript derived from the cells transfected with the NEIL1-c.936A type vector, but not from those with the NEIL1-c.936G type vector, contained the 160-bp intron 10 sequence (Figure 2D). These results indicate that the c.936G>A change caused the splicing abnormality. This abnormal splicing pattern leads to the replacement of the 78 aa C-terminus with 25 unrelated amino acids, resulting in the deletion of part of the nuclear localization signal (NLS). As the NEIL1 protein has been reported to be localized in the cell nucleus (20,21), we investigated whether the structural change resulting from the c.936G>A mutation actually affected subcellular localization. Wild-type and truncated-type NEIL1 cDNA fused with the FLAG sequence at the C-terminus were inserted into pcDNA3.1 mammalian expression vectors, and then transiently transfected into the NCI-H1299 cell line. The presence of exogenous NEIL1-FLAG proteins in the transfected cells was then examined using fluorescence microscopy (Figure 3). Consistent with previous results (20,21), the wild-type NEIL1-FLAG protein was localized in the nucleus; however, the truncated-type NEIL1-FLAG protein was localized in the cytoplasm. We also evaluated the subcellular localization of p.Arg334Gly-type protein in the same experimental design, however, the protein was localized in the nucleus (Figure 3). These results indicate that the c.936G>A-type truncated NEIL1 protein, lacking an NLS, is localized in the cytoplasm, unlike the nuclear localization of the wild-type NEIL1 protein, suggesting that the excisional repair ability of the truncated-type NEIL1 protein is impaired, preventing oxidatively damaged bases in nuclear DNA from being corrected.

Reduction in NEIL1 expression in gastric cancer

We next assessed the levels of NEIL1 mRNA expression in 13 primary gastric cancers and corresponding non-cancerous mucosae by QRT-PCR using the *PBGD* housekeeping gene as a control. The ratio of the NEIL1 mRNA expression level in the tumor compared with the corresponding non-cancerous tissue (T/N ratio) was calculated in each case (Figure 4). Six out of 13 (46%) of the primary gastric cancers exhibited a

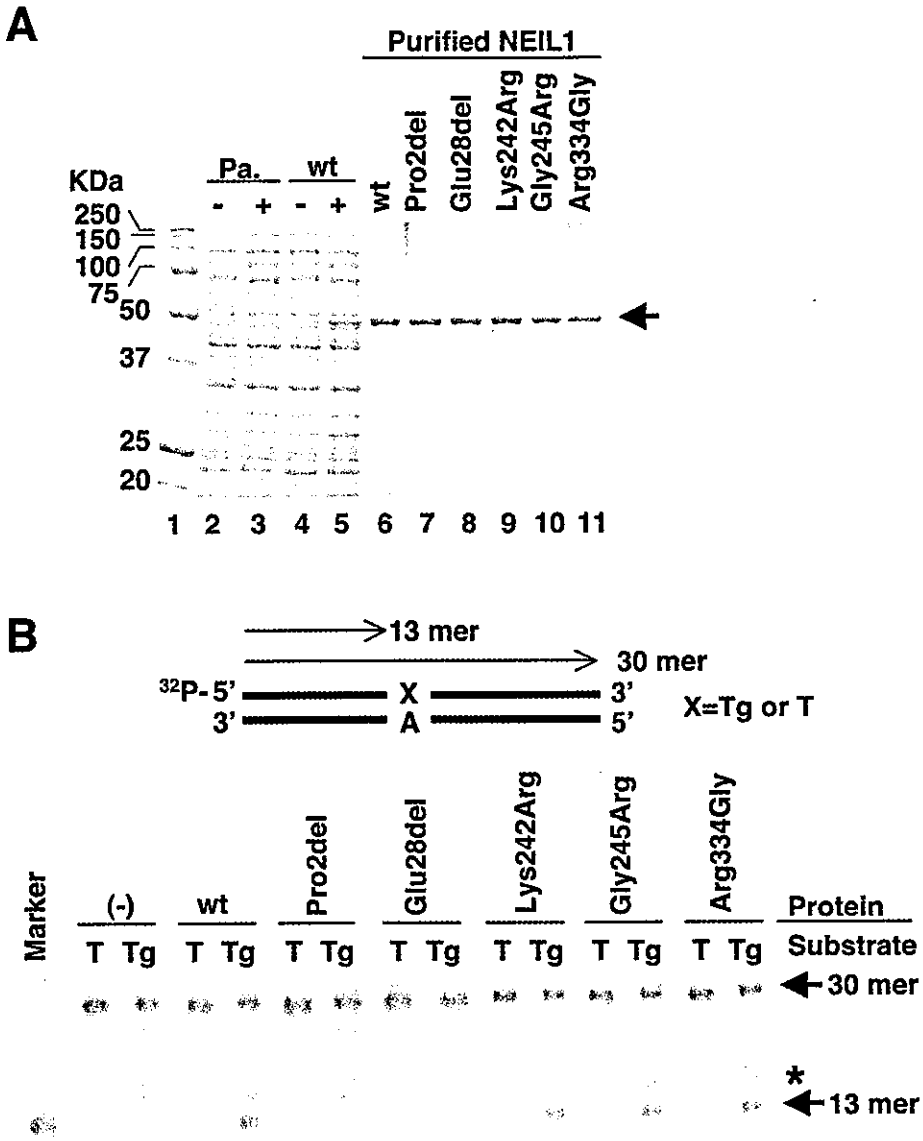

C

NEIL1 protein	% incision (average ± S.D.)
wt	33.4 ± 1.01
Pro2del	4.6 ± 0.16
Glu28del	7.7 ± 0.10
Lys242Arg	30.2 ± 4.42
Gly245Arg	32.8 ± 0.23
Arg334Gly	32.5 ± 1.21

Fig. 1. Comparison of the cleavage activity toward double-stranded DNA containing a Tg:A mispair among NEIL1 variant proteins. (A) Purification of recombinant NEIL1 proteins resolved by PAGE and stained with Coomassie Brilliant Blue. NEIL1 protein tagged with His_6 at its C-terminus was prepared according to the pET System protocol. Lysates of *E.coli* culture with/without expression of wild-type (wt) NEIL1 protein (lanes 2–5) and purified various NEIL1 proteins (lanes 6–11) are shown. Pa. (lanes 2 and 3) and wt (lanes 4 and 5) indicate the transformation of the host cells with parental pET25b(+) and *NEIL1* cDNA-containing pET25b(+) vector, respectively. – and + mean the absence and presence of IPTG induction, respectively. The NEIL1-His_6 protein band is indicated. (B) Cleavage activity of NEIL1 variant proteins toward double-stranded DNA containing a Tg:A mispair. Various types of NEIL1 proteins and a ^{32}P-labeled double-stranded oligonucleotide containing or not containing a single 5*R*,6*S*-Tg:A mispair were incubated and subjected to 20% PAGE. A ^{32}P-labeled 13mer oligonucleotide was used as a size marker for the cleaved products. A representative result is shown in the panel. (-) at the top of the panel indicates no addition of NEIL1 protein. The intact 30mer and cleaved 13mer oligonucleotides are indicated by the arrows. The band with an asterisk in the lane of the Tg substrate is an oligonucleotide impurity. (C) The percentage of cleaved products per total under conditions of 37°C for 15 min was calculated as % incision and listed.

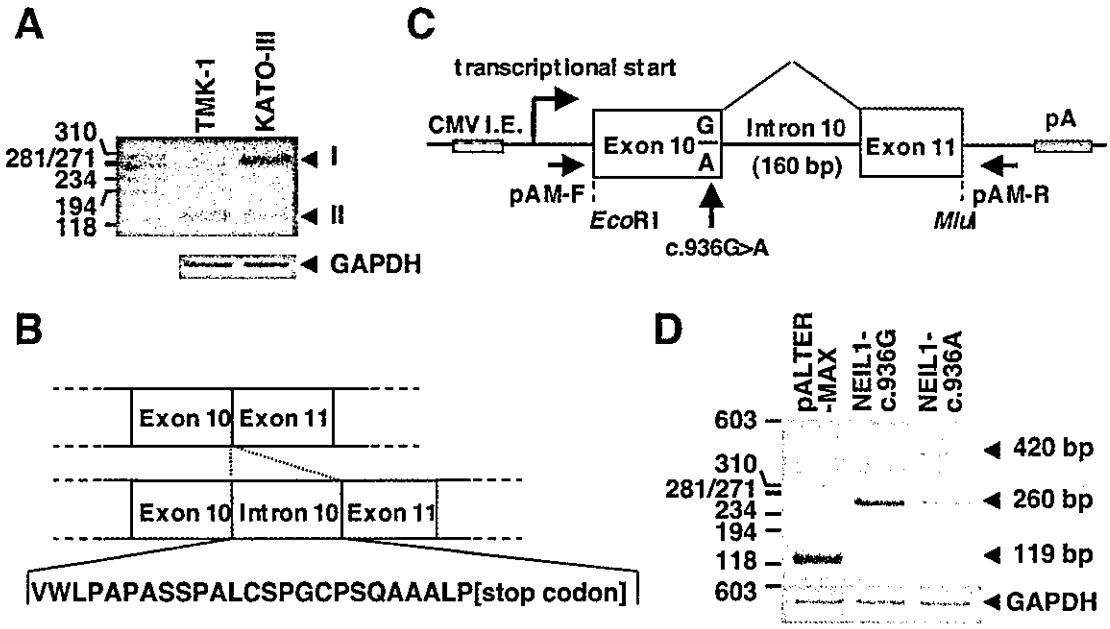

Fig. 2. Detection of the NEIL1 splicing abnormality due to the c.936G > A change by *in vivo* splicing assay. (A) Detection of the abnormally spliced product from KATO-III cell line by RT-PCR analysis. The genotypes of TMK-1 and KATO-III cells are homozygous for the c.936G allele and heterozygous for the c.936G and c.936A alleles, respectively. Expression of the NEIL1 mRNA transcript was examined using the primers located in exons 10 and 11. GAPDH expression was also examined. The band detected by electrophoresis was excised from the gel and directly sequenced. Bands indicated by arrowheads I and II are PCR products retaining or not retaining intron 10, respectively. (B) Diagram showing the polypeptide sequence translated from the read-through transcript of intron 10. (C) Schema of a part of pALTER-MAX expression vectors containing exon 10, intron 10 and exon 11 of the *NEIL1* gene. (D) *In vivo* splicing assay. The NEIL1-c.936G and -c.936A type expression vectors were transiently transfected into the NCI-H1299 cell line. At 24 h post-transfection, the cells were harvested, and RT-PCR was performed using the set of primers pAM-F/pAM-R, as indicated in (C), or a set of primers for GAPDH. PCR products were fractionated by agarose gel electrophoresis, and each band was directly sequenced. The 119-, 260- and 420-bp products correspond to a vector sequence without *NEIL1*, a *NEIL1* sequence without intron 10, and a *NEIL1* sequence with intron 10, respectively.

reduction in NEIL1 expression (0.5 > T/N ratio). A Wilcoxon signed-ranks test also showed that the NEIL1 mRNA level in the cancer tissue was significantly lower than that in the non-cancerous tissue ($P < 0.01$). A significant reduction in NEIL1 expression in the cancer tissue compared with the non-cancerous tissue was also observed when *GAPD* was used as the control housekeeping gene (data not shown). The level of NEIL1 expression in KATO-III cells carrying the c.936G > A mutation was less than one-tenth lower than that in the non-cancerous gastric tissue sample from case no. 1. These results indicate that NEIL1 expression may be reduced in some primary gastric cancers, although the underlying mechanism of this phenomenon is presently unknown.

Discussion

Three mutations and two genetic polymorphisms in the *NEIL1* gene locus were identified in the present study. When the Tg DNA glycosylase activity was compared among six types of recombinant NEIL1 proteins, p.Glu28del-type NEIL1, first identified in a primary gastric cancer, was found to exhibit an extremely low activity level. Moreover, the c.936G > A truncated NEIL1 protein, first detected in the KATO-III cell line, was shown to be associated with a splicing abnormality using an *in vivo* splicing assay. In contrast to the results for the wild-type NEIL1 protein, an immunofluorescence analysis showed that the c.936G > A-type truncated NEIL1 protein was localized in the cytoplasm, not the nucleus, suggesting that the truncated protein's ability to correct nuclear DNA damage via its excisional repair ability was likely to be impaired. An expression analysis revealed that NEIL1 mRNA expression was reduced in six of 13 (46%) of the primary gastric cancer specimens that were examined. These results suggest that low NEIL1 activities arising from mutations and reductions in expression may be involved in the pathogenesis of a subset of gastric cancers.

In this study, the NEIL1-p.Glu28del-type protein resulting from the c.82_84delGAG mutation was shown to exhibit a greatly reduced ability to cleave a double-stranded oilognucleotide containing a single *5R*,*6S*-Tg:A mispair. As mammalian NEIL1 protein has been shown to efficiently excise the substrate (23,26), the assay system used in this study was expected to be adequate to determine the level of the NEIL1 protein's repair ability. As expected, the repair ability of the p.Glu28del-type protein as well as the p.Pro2del-type protein, which is known to be an inactive form, was lower than that of the wild-type protein. However, the reason for the reduction in the repair ability was unclear, because the Glu28 residue is not located in a domain that is known to be necessary for the protein's repair function. The Glu28 residue may play an important role in the recognition of the DNA substrate, or some other related function. In the future, a crystal structure analysis of the NEIL1 protein alone and covalently complexed with DNA, in conjunction with the present finding that the p.Glu28del-type protein exhibited an extremely low activity level, would contribute to establishing further correlations between the structure and repair function of the NEIL1 protein.

The c.936G > A mutation caused a splicing abnormality that led to the production of an aberrant mRNA transcript encoding

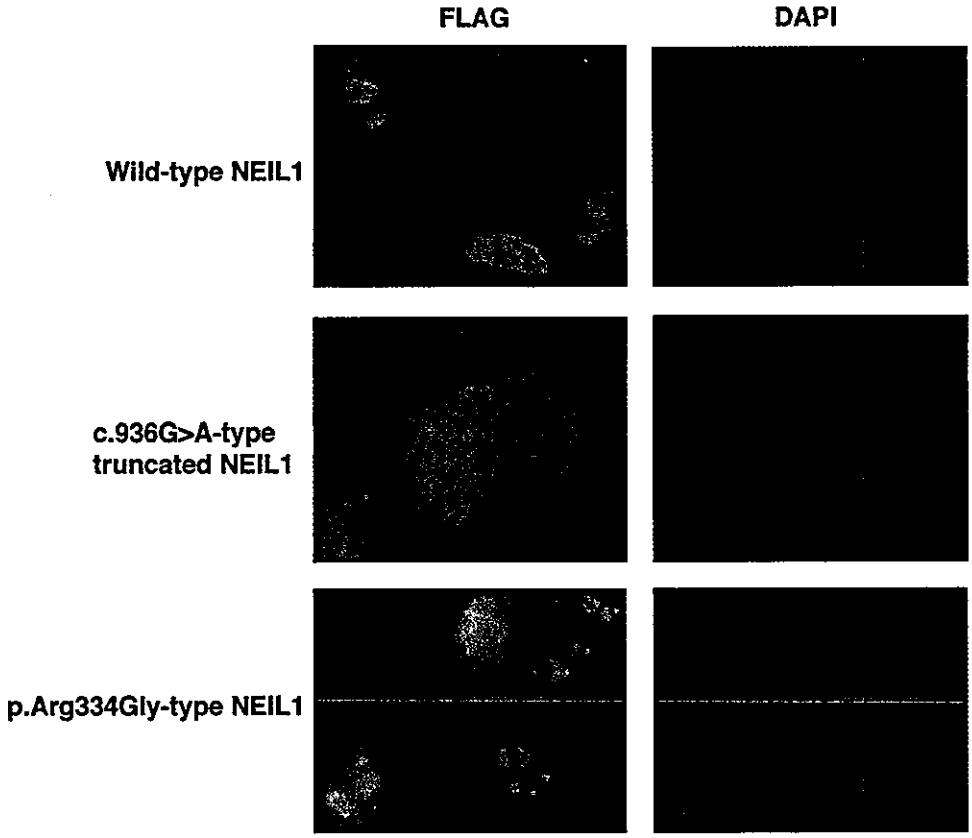

Fig. 3. The distinct subcellular localization of the wild- and mutant-type of NEIL1 protein. The wild-type and mutant-type NEIL1 with the FLAG epitope tag at the C-terminus were expressed in NCI-H1299 cells and stained with anti-FLAG M2 as the first antibody and FITC-conjugated anti-mouse IgG as the second antibody. The immunofluorescence microscopic image of FITC (green)-stained cells showed the localization of exogenous NEIL1 protein. The nuclei were counterstained with DAPI (blue).

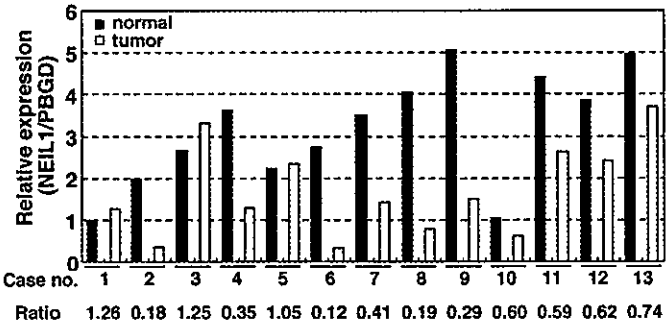

Fig. 4. NEIL1 expression in gastric cancer and corresponding non-cancerous tissue. Expression of the NEIL1 mRNA transcript was measured by QRT-PCR. The relative amounts of NEIL1 transcript were standardized according to those of the PBGD transcript. The relative expression of each sample was calculated by comparing the expression of non-cancerous gastric tissue in a primary gastric cancer patient (case no. 1). The T/N ratio is shown below the case number.

a truncated NEIL1 protein. Unlike the wild-type protein, the truncated NEIL1 protein was not localized in the nucleus, suggesting that the c.936G>A-type truncated protein could not repair nuclear DNA. KATO-III cells carrying this c.936G>A mutation also showed a reduction in NEIL1 mRNA expression, agreeing with the observation that NEIL1 mRNA expression was reduced in some primary gastric cancers in the present study. Thus, both genetic alterations may contribute to the low NEIL1 activity in the KATO-III cell line.

Regarding the prevalence of somatic mutations in human gastrointestinal cancer, Wang *et al.* (33) reported that only three non-synonymous somatic mutations, each in a different gene, were identified in ~3.2 Mb of coding colon cancer DNA, containing 1811 exons from 470 genes. Considering this prevalence, the observation of three *NEIL1* mutations in this study implies a relatively high prevalence of *NEIL1* somatic mutations in gastric cancer. Gastric cells with a *NEIL1* somatic mutation may have been selected during tumorigenesis. However, as we did not compare the prevalence of the *NEIL1* mutation in a variety of human cancers, it is unknown whether its prevalence in gastric cancer is significantly higher than in other cancers. We are planning to investigate this issue in the near future.

A reduction in the DNA repair function of the NEIL1 protein in human cells, particularly, where severe oxidative stress is present, could lead to a high level of accumulated oxidative DNA damage. This situation might lead to an increase in the incidence of gene mutation in the cells. Moreover, a 20–35% reduction in the repair capacity of cells has been associated with a 4–6-fold higher risk of developing cancer (34). Thus, it is suggested that low NEIL1 activities caused by mutations and reduced mRNA expression may contribute to the alteration of genes involved in gastric carcinogenesis in a subset of gastric cancers.

Acknowledgements

We thank Dr M.Takao of the Tohoku University, Sendai, Japan, for valuable advice on the expression of the NEIL1 protein, Dr Y.Gao of the Hamamatsu University School of Medicine, Japan, for instruction on the use of the Light-Cycler instrument, and Ms C.Tatebayashi of Hamamatsu University School of Medicine for her technical assistance. This work was supported in part by a Grant-in-Aid from the Ministry of Health, Labour and Welfare for the 2nd-term Comprehensive 10-Year Strategy for Cancer Control and from the Ministry of Education, Culture, Sports, Science and Technology of Japan for Scientific Research on Priority Area and the 21st century COE program 'Medical Photonics'.

References

1. Beckman,K.B. and Ames,B.N. (1997) Oxidative decay of DNA. *J. Biol. Chem.*, **272**, 19633–19636.
2. Wallace,S.S. (2002) Biological consequences of free radical-damaged DNA bases. *Free Radic. Biol. Med.*, **33**, 1–14.
3. Kasai,H. and Nishimura,S. (1991) Formation of 8-hydroxyguanosine in DNA by oxygen radicals and its biological significance. In Sies,H. (ed.) *Oxidative Stress: Oxidants and Antioxidants*. Academic Press, London, pp. 99–116.
4. Aburatani,H., Hippo,Y., Ishida,T. *et al.* (1997) Cloning and characterization of mammalian 8-hydroxyguanine-specific DNA glycosylase/apurinic, apyrimidinic lyase, a functional *mutM* homologue. *Cancer Res.*, **57**, 2151–2156.
5. Aspinwall,R., Rothwell,D.G., Roldan-Arjona,T. *et al.* (1997) Cloning and characterization of a functional human homolog of *Escherichia coli* endonuclease III. *Proc. Natl Acad. Sci. USA*, **94**, 109–114.
6. Lu,R., Nash,H.M. and Verdine,G.L. (1997) A mammalian DNA repair enzyme that excises oxidatively damaged guanines maps to a locus frequently lost in lung cancer. *Curr. Biol.*, **7**, 397–407.
7. Radicella,J.P., Dherin,C., Desmaze,C., Fox,M.S. and Boiteux,S. (1997) Cloning and characterization of *hOGG1*, a human homolog of the *OGG1* gene of *Saccharomyces cerevisiae*. *Proc. Natl Acad. Sci. USA*, **94**, 8010–8015.
8. Bjoras,M., Luna,L., Johnsen,B., Hoff,E., Haug,T., Rognes,T. and Seeberg,E. (1997) Opposite base-dependent reactions of a human base excision repair enzyme on DNA containing 7,8-dihydro-8-oxoguanine and abasic sites. *EMBO J.*, **16**, 6314–6322.
9. Roldan-Arjona,T., Wei,Y., Carter,K.C., Klungland,A., Anselmino,C., Wang,R., Augustus,M. and Lindahl,T. (1997) Molecular cloning and functional expression of a human cDNA encoding the antimutator enzyme 8-hydroxyguanine-DNA glycosylase. *Proc. Natl Acad. Sci. USA*, **94**, 8016–8020.
10. Shinmura,K., Kasai,H., Sasaki,A., Sugimura,H. and Yokota,J. (1997) 8-Hydroxyguanine (7,8-dihydro-8-oxoguanine) DNA glycosylase and AP lyase activities of hOGG1 protein and their substrate specificity. *Mutat. Res.*, **385**, 75–82.
11. Ikeda,S., Biswas,T., Roy,R., Izumi,T., Boldogh,I., Kurosky,A., Sarker,A.H., Seki,S. and Mitra,S. (1998) Purification and characterization of human NTH1, a homolog of *Escherichia coli* endonuclease III. Direct identification of Lys-212 as the active nucleophilic residue. *J. Biol. Chem.*, **273**, 21585–21593.
12. Shinmura,K. and Yokota,J. (2001) The *OGG1* gene encodes a repair enzyme for oxidatively damaged DNA and is involved in human carcinogenesis. *Antioxid. Redox Signal.*, **3**, 597–609.
13. Kohno,T., Shinmura,K., Tosaka,M., Tani,M., Kim,S.R., Sugimura,H., Nohmi,T., Kasai,H. and Yokota,J. (1998) Genetic polymorphisms and alternative splicing of the *hOGG1* gene, that is involved in the repair of 8-hydroxyguanine in damaged DNA. *Oncogene*, **16**, 3219–3225.
14. Audebert,M., Chevillard,S., Levalois,C. *et al.* (2000) Alterations of the DNA repair gene *OGG1* in human clear cell carcinomas of the kidney. *Cancer Res.*, **60**, 4740–4744.
15. Hyun,J.W., Choi,J.Y., Zeng,H.H., Lee,Y.S., Kim,H.S., Yoon,S.H. and Chung,M.H. (2000) Leukemic cell line, KG-1 has a functional loss of hOGG1 enzyme due to a point mutation and 8-hydroxydeoxyguanosine can kill KG-1. *Oncogene*, **19**, 4476–4479.
16. Bruner,S.D., Norman,D.P. and Verdine,G.L. (2000) Structural basis for recognition and repair of the endogenous mutagen 8-oxoguanine in DNA. *Nature*, **403**, 859–866.
17. Sugimura,H., Kohno,T., Wakai,K. *et al.* (1999) *hOGG1* Ser326Cys polymorphism and lung cancer susceptibility. *Cancer Epidemiol. Biomarkers Prev.*, **8**, 669–674.
18. Goode,E.L., Ulrich,C.M. and Potter,J.D. (2002) Polymorphisms in DNA repair genes and associations with cancer risk. *Cancer Epidemiol. Biomarkers Prev.*, **11**, 1513–1530.
19. Hazra,T.K., Izumi,T., Boldogh,I., Imhoff,B., Kow,Y.W., Jaruga,P., Dizdaroglu,M. and Mitra,S. (2002) Identification and characterization of a novel human DNA glycosylase for repair of cytosine-derived lesions. *Proc. Natl Acad. Sci. USA*, **99**, 3523–3528.
20. Takao,M., Kanno,S., Kobayashi,K., Zhang,Q.M., Yonei,S., van der Horst,G.T. and Yasui,A. (2002) A back-up glycosylase in *Nth1* knock-out mice is a functional Nei (endonuclease VIII) homologue. *J. Biol. Chem.*, **277**, 42205–42213.
21. Morland,I., Rolseth,V., Luna,L., Rognes,T., Bjoras,M. and Seeberg,E. (2002) Human DNA glycosylases of the bacterial Fpg/MutM superfamily: an alternative pathway for the repair of 8-oxoguanine and other oxidation products in DNA. *Nucleic Acids Res.*, **30**, 4926–4936.
22. Bandaru,V., Sunkara,S., Wallace,S.S. and Bond,J.P. (2002) A novel human DNA glycosylase that removes oxidative DNA damage and is homologous to *Escherichia coli* endonuclease VIII. *DNA Rep.*, **1**, 517–529.
23. Rosenquist,T.A., Zaika,E., Fernandes,A.S., Zharkov,D.O., Miller,H. and Grollman,A.P. (2003) The novel DNA glycosylase, NEIL1, protects mammalian cells from radiation-mediated cell death. *DNA Rep.*, **2**, 581–591.
24. Kroeger,K.M., Hashimoto,M., Kow,Y.W. and Greenberg,M.M. (2003) Cross-linking of 2-deoxyribonolactone and its beta-elimination product by base excision repair enzymes. *Biochemistry*, **42**, 2449–2455.
25. Dou,H., Mitra,S. and Hazra,T.K. (2003) Repair of oxidized bases in DNA bubble structures by human DNA glycosylases NEIL1 and NEIL2. *J. Biol. Chem.*, **278**, 49679–49684.
26. Miller,H., Fernandes,A.S., Zaika,E., McTigue,M.M., Torres,M.C., Wente,M., Iden,C.R. and Grollman,A.P. (2004) Stereoselective excision of thymine glycol from oxidatively damaged DNA. *Nucleic Acids Res.*, **32**, 338–345.
27. Baik,S.C., Youn,H.S., Chung,M.H., Lee,W.K., Cho,M.J., Ko,G.H., Park,C.K., Kasai,H. and Rhee,K.H. (1996) Increased oxidative DNA damage in *Helicobacter pylori*-infected human gastric mucosa. *Cancer Res.*, **56**, 1279–1282.
28. Farinati,F., Cardin,R., Degan,P., Rugge,M., Mario,F.D., Bonvicini,P. and Naccarato,R. (1998) Oxidative DNA damage accumulation in gastric carcinogenesis. *Gut*, **42**, 351–356.
29. Tredaniel,J., Boffetta,P., Buiatti,E., Saracci,R. and Hirsch,A. (1997) Tobacco smoking and gastric cancer: review and meta-analysis. *Int. J. Cancer*, **72**, 565–573.
30. Kiyokawa,E., Takai,S., Tanaka,M., Iwase,T., Suzuki,M., Xiang,Y.Y., Naito,Y., Yamada,K., Sugimura,H. and Kino,I. (1994) Overexpression of ERK, an EPH family receptor protein tyrosine kinase, in various human tumors. *Cancer Res.*, **54**, 3645–3650.
31. Takezaki,T., Gao,C.M., Wu,J.Z. *et al.* (2002) *hOGG1* Ser(326)Cys polymorphism and modification by environmental factors of stomach cancer risk in Chinese. *Int. J. Cancer*, **99**, 624–627.
32. Chabot,B. (1996) Directing alternative splicing: cast and scenarios. *Trends Genet.*, **12**, 472–478.
33. Wang,T.L., Rago,C., Silliman,N., Ptak,J., Markowitz,S., Willson,J.K., Parmigiani,G., Kinzler,K.W., Vogelstein,B. and Velculescu,V.E. (2002) Prevalence of somatic alterations in the colorectal cancer cell genome. *Proc. Natl Acad. Sci. USA*, **99**, 3076–3080.
34. Mohrenweiser,H.M. and Jones,I.M. (1999) Variation in DNA repair is a factor in cancer susceptibility: a paradigm for the promises and perils of individual and population risk estimation? *Mutat. Res.*, **400**, 15–24.

Received May 1, 2004; revised July 29, 2004; accepted August 10, 2004

High Lactate Dehydrogenase Isoenzyme 1 in a Patient with Malignant Germ Cell Tumor Is Attributable to Aberrant Methylation of the *LDHA* Gene, *Jinko Ishikawa,*[1] *Terumi Taniguchi,*[1] *Hitomi Higashi,*[1] *Katsutoshi Miura,*[2] *Kazuya Suzuki,*[3] *Akihiro Takeshita,*[1] *and Masato Maekawa*[1]* ([1] Department of Laboratory Medicine, [2] Department of Pathology, and [3] First Department of Surgery, Hamamatsu University School of Medicine, Hamamatsu 431-3192, Japan; * author for correspondence: fax 81-53-435-2794, e-mail mmaekawa@hama-med.ac.jp)

Lactate dehydrogenase (LD; EC 1.1.1.27) isoenzymes are formed by random combinations of two different subunits encoded by structurally distinct genes, *LDHA* and *LDHB (1)*. Expression of mammalian *LDHA* and *LDHB* is regulated during development and is tissue specific; therefore, alterations in the serum LD isoenzyme pattern serve as indicators of pathologic conditions and cancer development *(2)*. Different phenotypes of LD isoenzyme patterns in cancer patients may originate from changes in expression of *LDHA* or *LDHB* caused by other regulatory genes or promoter methylation or from mutations involving deletions, duplications, or increased copy numbers. We previously observed in a retinoblastoma cell line a high proportion of LD1 with an extra band that migrated between LD2 and LD3. The unique LD isoenzyme pattern was attributable in part to transcriptional silencing by hypermethylation of the *LDHA* promoter *(3)*. We also found that the increased concentrations of electrophoretically slow-moving LD isoenzymes in many gastric cancer cell lines are attributable to transcriptional silencing of *LDHB* expression by aberrant promoter methylation *(4)*.

We recently encountered a male patient with mediastinal germ cell tumor who showed high serum LD activity and high LD1 isoenzyme activity. In germ cell tumors, increased LD1 concentrations often correlate with total copy number for the short arm of chromosome 12, which is where *LDHB* is located *(5)*, but not all germ cell tumors show this increased copy number for chromosome 12. We therefore hypothesized that the high LD1 isoenzyme activity could be caused by aberrant methylation of the *LDHA* promoter.

The patient, a 21-year-old man, was admitted to our hospital because of fever and abnormal chest x-ray results. Laboratory tests revealed increased serum LD activity (299 U/L; reference interval, 101–193 U/L). Serum α-fetoprotein was increased to 2535 μg/L (reference interval <10 μg/L). The LD profiles included increased LD1 (49%) and a high LD1/LD2 ratio (2.2; Table 1). Chest x-ray examination revealed a mediastinal tumor. A pathology examination revealed that the tumor consisted of a combined malignant germ cell tumor (yolk sac tumor plus embryonal carcinoma plus dysgerminoma) with a focal rhabdomyosarcoma component arising from a mature cystic teratoma of the mediastinum (size, 8 × 8 × 4.8 cm). After surgical resection of the pulmonary metastasis, total LD activity decreased, but the LD isoenzyme pattern with high LD1 activity remained. After surgical resection of the primary tumor followed by high-dose chemotherapy, both the total LD activity and the LD isoenzyme pattern returned to normal (Table 1).

LD activity was measured by spectrophotometric assay on a Hitachi 7350 automated biochemistry analyzer (Hitachi High Technologies). Assay conditions were based on the method recommended by the Japanese Society of Clinical Chemistry *(6)*. LD isoenzymes in serum were separated electrophoretically with Titan III support medium (Helena Laboratory).

Genomic DNA was extracted from the formalin-fixed, paraffin-embedded specimens of the surgically resected pulmonary metastasis and the primary mediastinal tumor with DNA isolation reagents (DNeasy Tissue Kit; Qiagen). For methylation analysis, we used methylation-specific PCR (MSP) *(7)*. The sequences of primers specific for the methylated allele of *LDHA* were 5′-CGATTTCGGATTTTATTGTTACGC-3′ (forward) and 5′-CGCCCATCCCTCTACCCGTACG-3′ (reverse); those for the unmethylated allele were 5′-TATTTAAGTAGGGGTTGAAAGTTT-3′ (forward) and 5′-ACCTCAAATTTTACACCACCG-3′ (reverse; see Fig. 1 in the Data Supplement that accompanies the online version of this Technical Brief at http://www.clinchem.org/content/vol50/issue10/). The MSP-amplified products were confirmed by single-strand DNA conformation polymorphism (SSCP) analysis *(8)* and DNA sequencing analysis.

Table 1. Patient's lactate dehydrogenase profile and α-fetoprotein concentrations on various dates during 2003.

Test	Reference interval	Jan. 16	Feb. 11[a]	Feb. 27	March 18	June 12	Aug. 5[b]	Oct. 1[c]
LD, U/L	101–193	299	307	166	143	177	161	110
LD1, %	20.0–31.0	48.6		22.9		39.8		23.2
LD2, %	28.8–37.0	22.0		23.5		32.7		35.2
LD3, %	21.5–27.6	13.8		17.5		16.0		25.3
LD4, %	6.3–12.4	7.8		13.0		4.8		9.1
LD5, %	5.4–13.2	7.8		23.1		6.8		7.2
LD1/LD2	0.60–0.93	2.2		1.0		1.2		0.7
AFP,[d] μg/L	<10	2535	372		43	229	92	5

[a] After resection of pulmonary metastasis of the tumor and chemotherapy.
[b] After high-dose chemotherapy.
[c] After surgical resection of the primary tumor.
[d] AFP, α-fetoprotein.

MSP-SSCP analysis was performed with 15% nondenaturing polyacrylamide gels and silver-staining detection (Daiichi Pure Chemicals). DNA sequencing analysis was performed with a BigDye Terminator Cycle Sequencing FS Ready Reaction Kit and a PRISM 310 Genetic Analyzer (PE Applied Biosystems).

For mutation analysis, all seven exons of the *LDHA* and *LDHB* genes were investigated by PCR-SSCP and DNA sequencing analysis to detect mutations *(9, 10)*. To examine gene amplification, we used two pairs of PCR primers to amplify short fragments of the genomic DNAs of *LDHA* and *LDHB*. These primers, the same ones used for the mutation analysis described above, amplified exon 2 *(9, 10)*. We performed 25, 30, and 35 cycles of PCR and analyzed the *LDHA* and *LDHB* genes separately. PCR products were separated by electrophoresis on 1.5% agarose gels and visualized by ethidium bromide staining and ultraviolet transillumination. Stained bands were analyzed densitometrically with Cool Saver imaging software (ATTO Corp.).

Methylation of the *LDHA* promoter was detected by MSP in three representative tumor regions (1T, 2T, and 3T), with trace bands of unmethylated allele. In the nontumorous region (nontumor control), however, only the unmethylated promoter was observed (Fig. 1A). Products amplified from tumor regions with methylated allele-specific primers showed SSCP patterns similar to the pattern from control methylated DNA with several additional bands or slight smearing. The differences probably originated from partially methylated DNAs that were methylated to various degrees at individual CpG sites. Products amplified from the nontumor control and tumor regions showed the same SSCP pattern as control unmethylated DNA (Fig. 1B). Sequence analysis revealed methylation of CpGs in the *LDHA* promoter region of methylated allele-specific PCR products from tumor regions. No methylation was observed in the unmethylated allele-specific PCR products from the nontumor control region (data not shown).

We did not detect any missense or nonsense mutations in the protein-coding exons and exon-intron boundaries of both the *LDHA* and *LDHB* genes in either the nontumor control or tumor specimens (data not shown). At different cycles of amplification for genomic DNAs of *LDHA* and *LDHB*, the *LDHA*/*LDHB* ratios in the nontumor control samples and the tumor region and the nontumor/tumor ratios in *LDHA* and *LDHB* products did not differ significantly (see Fig. 2 in the online Data Supplement). Therefore, amplification of *LDHB* and deletion of *LDHA* were possibly contradicted.

In mammals, DNA methylation usually occurs at CpG dinucleotides. Methylation is known to play a role in regulation of gene expression during cell development, X chromosome inactivation, genomic imprinting, and carci-

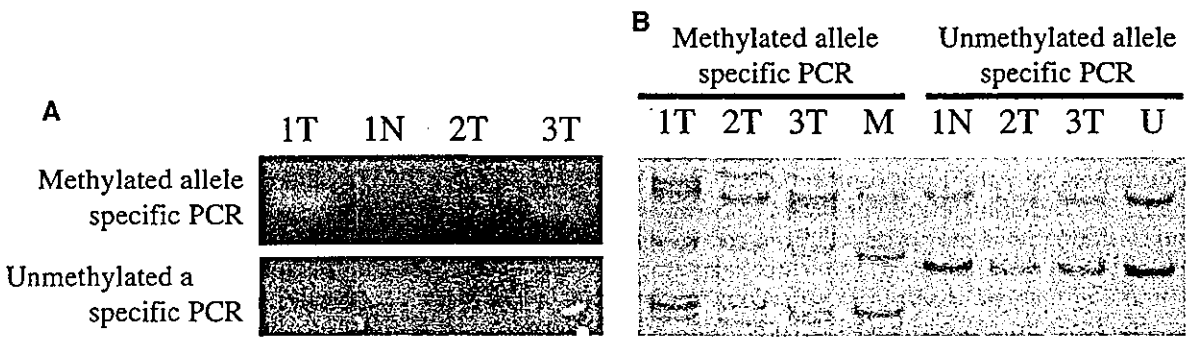

Fig. 1. Methylation analysis.

(*A*), results of bisulfite treatment and MSP analysis of the *LDHA* promoter in three tumor tissue sections (*T*) and one nontumor tissue section (*N*). (*B*), results of SSCP analysis of the above MSP-amplified products. SSCP was performed at 15 °C with 15% polyacrylamide gels. *U*, unmethylated control DNA; *M*, methylated control DNA.

nogenesis *(11, 12)*. In neoplastic cells, some usually unmethylated CpG islands in the promoter region become aberrantly methylated, and this leads to transcriptional silencing of various genes *(13)*. The human *LDHA* and *LDHB* genes both have CpG-rich regions in their promoters *(14)*.

In the patient described here, we observed that the promoter region around exon a of *LDHA* was aberrantly methylated. This might silence expression of the somatic *LDHA* gene, possibly leading to relative increases in LDHB protein concentrations and LD1 activity. We also found that increased concentrations of electrophoretically fast-moving LD isoenzymes in some types of cancer are the result of transcriptional silencing of *LDHA* expression as result of aberrant methylation of the *LDHA* promoter. Thus, as reported previously, enzyme abnormalities in tumors occasionally originate from aberrant methylation. Significant increases in LD1 and LD5 have been reported previously *(15, 16)*. The LD isoenzyme patterns in these patients could be the result of aberrant *LDHA* or *LDHB* methylation in cancer cells.

Human testicular germ-cell tumors are typically characterized by overrepresentation of 12p. These tumors were shown to contain striking amplification of a restricted region of 12p that included the K-*ras* protooncogene. Seminomas with this 12p amplification do not undergo apoptosis, and the tumor cells showed prolonged in vitro survival, as do seminoma cells with a mutated *ras* gene *(17)*. Indeed, high concentrations of LD1 may yield a better prognostic predictor for the patients with testicular germ cell tumors *(5, 18)*. Amplification of 12p is associated with poor prognosis, whereas methylation of *LDHA* may indicate a good prognosis. This issue should be addressed by investigating a large sample of patients with high LD1 attributable to amplification of *LDHB* or methylation of *LDHA*.

To our knowledge, this is the first reported case in which the specific LD isoenzyme pattern in serum was linked directly to promoter methylation. The next issue is whether methylation of the *LDHA* promoter is a common mechanism underlying increased LD1 concentrations in germ-cell tumors.

This research was supported in part by a Health and Labour Sciences Research Grant (H15-9) from the Ministry of Health, Labour and Welfare, Japan; by a Research on Cancer Prevention and Health Services Grant; and by a Grant-in-Aid for Scientific Research (13470518) from the Ministry of Education, Science, Sports, Culture and Technology, Japan.

References

1. Markert CL. Lactate dehydrogenase isozymes: dissociation and recombination of subunits. Science 1963;140:1329–30.
2. Maekawa M. Lactate dehydrogenase isoenzymes. J Chromatogr 1988;429: 373–98.
3. Maekawa M, Inomata M, Sasaki MS, Kenko A, Ushiama M, Sugano K, et al. Electrophoretic variant of lactate dehydrogenase isoenzyme and selective promoter methylation of the *LDHA* gene in a human retinoblastoma cell line. Clin Chem 2002;48:1938–45.
4. Maekawa M, Taniguchi T, Ishikawa J, Sugimura H, Sugano K, Kanno T. Promoter hypermethylation in cancer silences *LDHB*, eliminating lactate dehydrogenase isoenzymes 1–4. Clin Chem 2003;49:1518–20.
5. von Eyben FE. A systematic review of lactate dehydrogenase isoenzyme 1 and germ cell tumors. Clin Biochem 2001;34:441–54.
6. Japanese Society of Clinical Chemistry. Recommendation method for the measurement of human serum enzyme activity–lactate dehydrogenase. Jpn J Clin Chem 2004;33(Suppl):97a–115a.
7. Herman JG, Graff JR, Myohanen S, Nelkin BD, Baylin SB. Methylation-specific PCR: a novel PCR assay for methylation status of CpG islands. Proc Natl Acad Sci U S A 1996;93:9821–6.
8. Maekawa M, Sugano K, Kashiwabara H, Ushiama M, Fujita S, Yoshimori M, et al. DNA methylation analysis using bisulfite treatment and PCR-single-strand conformation polymorphism in colorectal cancer showing microsatellite instability. Biochem Biophys Res Commun 1999;262:671–6.
9. Maekawa M, Sudo K, Kobayashi A, Sugiyama E, Li SS, Kanno T. Fast-type electrophoretic variant of lactate dehydrogenase M(A) and comparison with other missense mutations in lactate dehydrogenase M(A) and H(B) genes. Clin Chem 1994;40:665–8.
10. Sudo K, Maekawa M, Kanno T, Li SS, Akizuki S, Magara T. Premature termination mutations in two patients with deficiency of lactate dehydrogenase H(B) subunit. Clin Chem 1994;40:1567–70.
11. Li E, Beard C, Jaenisch R. Role for DNA methylation in genomic imprinting. Nature 1993;366:362–5.
12. Jones PA. DNA methylation errors and cancer. Cancer Res 1996;56: 2463–7.
13. Baylin SB, Herman JG, Graff JR, Vertino PM, Issa JP. Alterations in DNA methylation: a fundamental aspect of neoplasia. Adv Cancer Res 1998;72: 141–96.
14. Bonny C, Goldberg E. The CpG-rich promoter of human LDH-C is differentially methylated in expressing and nonexpressing tissues. Dev Genet 1995;16: 210–7.
15. Kanowski D, Clague A. Increased lactate dehydrogenase isoenzyme-1 in a case of glucagonoma. Clin Chem 1994;40:158–9.
16. Yamauchi K, Igarashi F, Nakayama T, Yoshida Y, Eto H, Anzai H. A case of gallbladder carcinoma with sustaining high levels of serum lactate dehydrogenase isozyme 1. Jpn J Clin Chem 1991;20:162–7.
17. Roelofs H, Mostert MC, Pompe K, Zafarana G, van Oorschot M, van Gurp RJ, et al. Restricted 12p amplification and RAS mutation in human germ cell tumors of the adult testis. Am J Pathol 2000;157:1155–66.
18. von Eyben FE, de Graaff WE, Marrink J, Blaabjerg O, Sleijfer DT, Koops HS, et al. Serum lactate dehydrogenase isoenzyme 1 activity in patients with testicular germ cell tumors correlates with the total number of copies of the short arm of chromosome 12 in the tumor. Mol Gen Genet 1992;235: 140–6.

Previously published online at DOI: 10.1373/clinchem.2004.037739

Methylation of Mitochondrial DNA Is Not a Useful Marker for Cancer Detection

To the Editor:

The human mitochondrial (mt) DNA is small (16.5 kb) and encodes 13 respiratory chain subunits, 22 transfer RNAs, and 2 ribosomal RNAs. mtDNA is present at 1000–10 000 copies/cell, and the vast majority of these copies are identical (homoplasmic) at birth. A large number and wide variety of mtDNA mutations have been identified, and >200 disorders are associated with specific point mutations, single deletions, multiple deletions, or depletion of mtDNA *(1)*.

Several mtDNA mutations were recently found in human colorectal cancers and bladder, head and neck, and lung tumors *(2)*. Mutated mtDNA was detected in body fluids from patient with each type of the above cancers and was much more abundant than was mutated nuclear p53 DNA *(2)*. Aberrant DNA methylation has been identified as an important mechanism for inactivation of carcinogenesis-related genes in neoplasias *(3)*. By virtue of the clonal nature and high copy number of mtDNA, we hypothesized that methylation and mutations of mtDNA could be detected in body fluids and be useful as molecular markers for detection of cancer. In the present study, we focused on the aberrant methylation of mtDNA in cancer cell lines and tissue specimens from patients with gastrointestinal cancers.

The present study included 15 cancer cell lines and tissues from 31 patients with gastric cancer and 25 patients with colorectal cancer. The patients were similar to those who participated in our previous studies *(4)*. For the patients, both malignant and nonmalignant tissues were examined. Each patient consented to the experimental use and pathology examination of the specimens.

To examine methylation, we performed bisulfite-PCR–single-stranded DNA conformation polymorphism (SSCP) analysis as described previously *(4)*. Three pairs of primers based on GenBank accession no. NC_001807 were used for amplification of mtDNA. Primer pairs were as follows:

Sense, 5′-TAAGTTATTTTAGGGATAAT-3′ (nucleotides 2920–2941); antisense, 5′-ATCTTAACAAACCCTATTCTTA-3′ (3195–3216)

Sense,5′-TTGAGTTATGATATTAATTGGT-3′ (6725–6746); antisense, 5′-CATAATAAAAATAAACTACAAC-3′ (6999–7020)

Sense,5′-TTGGTTATTAATGGTATTGAAT-3′ (7884–7905); antisense, 5′-AAAAACAACTCATAAATACAAA-3′ (8041–8062).

In the 16.5-kb human mitochondrial genome there are 435 CpG sites and 4747 cytosines at non-CpG sites. The primers were selected to amplify the maximum number of CpG sites. PCR products were expected to contain 318 bp and 13 CpG sites, 317 bp and 13 CpG sites, and 200 bp and 11 CpG sites, respectively. PCR products were subjected to SSCP analysis and sequenced directly with a BigDye Terminator Cycle Sequencing FS Ready Reaction Kit and a PRISM 310 Genetic Analyzer (Applied Biosystems).

Bisulfite-PCR–SSCP analysis revealed only unmethylated bands for all analyzed samples. Several SSCP bands were analyzed by direct sequencing, and the lack of methylated DNA was confirmed. Therefore, we believe that methylation of mtDNA is a rare event in the regions we analyzed in cancer cell lines and tissues from patients with gastric and colorectal cancer.

CpG dinucleotides are pervasively underrepresented in all animal mito-

chondria but vary in frequency in fungal, protist, and plant mitochondrial genomes (5). The methylation-deamination-mutation scenario may not apply to mtDNA genomes because the necessary methylase is not produced by most invertebrates or the methylase does not or can not access mitochondria in vertebrates. In contrast, endogenous methylation of 5-methylcytosine has been reported in mtDNA of rodents and human fibroblasts in culture (6). In that study, ~2–5% of CCGG sites were fully methylated, suggesting that nuclear methylases enter a subset of the mitochondria. Whether mtDNA can be methylated remains controversial. In the present study we examined selective regions containing more CpG sites. For an exhaustive study targeting whole mtDNA sequences, procedures more effective than bisulfite modification should be developed.

In conclusion, hypermethylation of mtDNA occurs at a very low frequency and does not appear to be a sensitive marker for detection of cancer.

This research was supported in part by a Labour Sciences Research grant (H15-Cancer Prevention-9) and by a Grant-in-Aid for Scientific Research (14657625) from the Ministry of Education, Science, Sports, Culture and Technology of Japan.

References

1. Marcelino LA, Thilly WG. Mitochondrial mutagenesis in human cells and tissues. Mutat Res 1999;434:177–203.
2. Baylin SB, Herman JG, Graff JR, Vertino PM, Issa JP. Alterations in DNA methylation: a fundamental aspect of neoplasia. Adv Cancer Res 1998; 72:141–96.
3. Fliss MS, Usadel H, Caballero OL, Wu L, Buta MR, Eleff SM, et al. Facile detection of mitochondrial DNA mutations in tumors and bodily fluids. Science 2000;287:2017–9.
4. Maekawa M, Sugano K, Ushiama M, Fukayama N, Nomoto K, Kashiwabara H, et al. Heterogeneity of DNA methylation status analyzed by bisulfite-PCR-SSCP and correlation with clinico-pathological characteristics in colorectal cancer. Clin Chem Lab Med 2001;39:121–8.
5. Cardon LR, Burge C, Clayton DA, Karlin S. Pervasive CpG suppression in animal mitochondrial genomes. Proc Natl Acad Sci U S A 1994;91: 3799–803.
6. Shmookler Reis RJ, Goldstein S. Mitochondrial DNA in mortal and immortal human cells. Genome number, integrity, and methylation. J Biol Chem 1983;258:9078–85.

Masato Maekawa[1*]
Terumi Taniguchi[1]
Hitomi Higashi[1]
Haruhiko Sugimura[2]
Kokichi Sugano[3]
Takashi Kanno[1]

[1] *Department of Laboratory Medicine and*
[2] *First Department of Pathology Hamamatsu University School of Medicine Hamamatsu, Japan*

[3] *Oncogene Research Unit Cancer Prevention Unit Tochigi Cancer Center Research Institute Utsunomiya, Japan*

*Address correspondence to this author at: Department of Laboratory Medicine, Hamamatsu University School of Medicine, Hamamatsu 431-3192, Japan. Fax 81-53-435-2794; e-mail mmaekawa@hama-med.ac.jp.

DOI: 10.1373/clinchem.2004.035139

Clinical Chemistry 50:8
1322–1327 (2004)

Molecular Diagnostics and Genetics

Three-Dimensional Microarray Compared with PCR–Single-Strand Conformation Polymorphism Analysis/DNA Sequencing for Mutation Analysis of K-*ras* Codons 12 and 13

MASATO MAEKAWA,[1*] TOMONORI NAGAOKA,[1,3] TERUMI TANIGUCHI,[1] HITOMI HIGASHI,[1] HARUHIKO SUGIMURA,[2] KOKICHI SUGANO,[4] HIROYUKI YONEKAWA,[5] TAKATOMO SATOH,[3] TOSHINOBU HORII,[1] NAOHITO SHIRAI,[1] AKIHIRO TAKESHITA,[1] and TAKASHI KANNO[1]

Background: **We developed a rapid, precise, and accurate microarray-based method that uses a three-dimensional platform for detection of mutations.**
Methods: **We used the PamChip® microarray to detect mutations in codons 12 and 13 of K-*ras* in 15 cell lines and 81 gastric or colorectal cancer tissues. Fluorescein isothiocyanate-labeled PCR products were analyzed with the microarray. We confirmed the microarray results with PCR–single-strand conformation polymorphism (SSCP) analysis and DNA sequencing.**
Results: **We could correctly identify wild-type, heterozygous, and homozygous mutant genotypes with the PamChip microarray in <3.5 h. The array data were consistent with those of PCR-SSCP analysis and DNA sequencing. All 15 cell lines and 80 of 81 clinical cancer specimens (98.8%; 95% confidence interval, 96.4–100%) were genotyped accurately with the microarray, a rate better than that of direct DNA sequencing (38.9%) or SSCP (93.8%). Only one clinical specimen was misdiagnosed as homozygous for the wild-type allele. Densitometric analysis of SSCP bands indicated that the content of the mutant allele in the specimen was ~16%. The PamChip microarray could detect mutant alleles representing more than 25% of the SSCP band proportions. Therefore, the limit for detection of mutant alleles by the PamChip microarray was estimated to be 16–25% of the total DNA.**
Conclusions: **The PamChip microarray is a novel three-dimensional microarray system and can be used to analyze K-*ras* mutations quickly and accurately. The mutation detection rate was nearly 100% and was similar to that of PCR-SSCP together with sequencing analysis, but the microarray analysis was faster and easier.**

Microarray technologies were initially developed to study differential gene expression in complex populations of RNA in tissues. Microarrays used for such purposes have a high density of spots (*1*, *2*). Detection of single-nucleotide polymorphisms (SNPs) by microarrays is a versatile methodology that is suitable for high-throughput diagnostic procedures (*3*, *4*). SNP detection and genotyping have also been done by PCR–single-strand conformation polymorphism (PCR-SSCP) analysis, degenerate HPLC, PCR–restriction fragment length polymorphism analysis, DNA sequencing, TaqMan PCR, and the Invader assay (*5*). DNA microarrays have also been used for genotyping applications, including SNP typing, detection of genomic and somatic mutations, identification of microbes, and detection of allelic imbalances (*6–11*). Commercially available microarrays have features beyond simple passive hybridization, including microfabricated fluidic channels, electronic hybridization, novel posthybridization signaling steps, and flow-through dynamics (*12*, *13*).

Recently, PamGene International B.V. developed a novel three-dimensional flow-through platform that uses a porous aluminum oxide substrate as a solid support (*14*). Because the substrate has long branched capillaries,

[1] Department of Laboratory Medicine and [2] 1st Department of Pathology, Hamamatsu University School of Medicine, Hamamatsu, Japan.
[3] Genome Medical Business Division, OLYMPUS Corporation, Hachioji, Japan.,
[4] Oncogene Research Unit/Cancer Prevention Unit, Tochigi Cancer Center Research Institute, Utsunomiya, Japan.
[5] Scientific Equipment Group, OLYMPUS America, Inc., New York, NY.
*Address correspondence to this author at: Department of Laboratory Medicine, Hamamatsu University School of Medicine, Hamamatsu 431-3192, Japan. Fax 81-53-435-2794; e-mail mmaekawa@hama-med.ac.jp.
Received January 28, 2004; accepted May 17, 2004.
Previously published online at DOI: 10.1373/clinchem.2004.032060

the reactive surface of this material is several-hundred-fold greater than that of a two-dimensional surface. Therefore, the flow-through microarray reduces hybridization times and increases signal and signal-to-noise ratios. This unique platform technology has been used by PamGene International B.V. and OLYMPUS Corporation to develop the PamChip® microarray and FD10 microarray system. The PamChip microarray has a disposable housing optimized for flow-through hybridization of samples. The hybridization is performed by repeated pumping of the sample solution up and down through the substrate. FD10 is an integrated PamChip microarray system that has solution-driven incubation and image acquisition functions with the ability to analyze and process four arrays simultaneously as well as optimized software for analysis. This system has already been used for gene expression profiling *(15)*.

K-*ras* is an oncogene in which various point mutations are frequently detected in cancers of the digestive organs. The mutations are clustered in a very narrow region, codons 12 and 13 *(16)*. The mutation sites in codon 12 are considered a mutational hot spot in carcinogenesis, which makes K-*ras* a promising candidate for mutation screening with microarray technologies.

Here we describe a rapid, precise, and accurate microarray system that uses the three-dimensional platform technology for mutation detection. Retrospective and/or comparative analyses were performed for mutations in codons 12 and 13 of K-*ras*.

Materials and Methods

SAMPLES AND DNA ISOLATION

Cancer cell lines were obtained from the Japanese Cell Resource Bank (COLO320, MKN1, MKN7, MKN28, MKN45, MKN74, KATOIII, A431, and LU65) and from the American Type Culture Collection (SW1116). The NEDATE cell line was established at the National Cancer Center Hospital. The C-1 and PSN1 cell lines were kindly supplied by the Pathology Division of the National Cancer Center Research Institute. Lymphoblastoid cell lines (TK6 and WTK-1) were obtained from the National Institute of Health Science. Genomic DNA was extracted from 15 cell lines as described previously *(17, 18)*.

DNA samples extracted from gastric or colorectal cancer tissues and corresponding healthy mucosae were selected from DNA stocks at Hamamatsu University School of Medicine, National Cancer Center Hospital, and Tochigi Cancer Center Hospital by K-*ras* mutation typing based on previously performed PCR-SSCP analysis. The experimental design was approved by the Committee for Genetic Analysis at Hamamatsu University School of Medicine.

PCR-SSCP ANALYSIS AND DIRECT SEQUENCING

The PCR primers used have been described previously *(19)*. These primers amplify a 108-bp fragment containing codons 12 and 13. PCR was performed with *Ex*Taq (TaKaRa), and the amplified products were sequenced directly or subjected to SSCP analysis on 10% nondenaturing polyacrylamide gels (Daiichi Pure Chemicals) *(20)*. Occasionally, extra bands (possibly mutated) detected by SSCP were excised from gels, reamplified, and sequenced. PCR products showing mobility shifts were then sequenced directly with the BigDye Terminator Cycle Sequencing FS Ready Reaction Kit and ABI PRISM 310 Genetic Analyzer (Applied Biosystems).

MICROARRAY ANALYSIS

Oligonucleotide probes (17mers) were designed to detect K-*ras* mutations (see Table 1 in the Data Supplement that accompanies the online version of this article at http://www.clinchem.org/content/vol50/issue8/) and spotted on PamChip microarrays. The layout of the PamChip microarrays is shown in Fig. 1. Wild-type probes for codons 12 and 13 (GGTGGC; shaded circles in Fig. 1) and eight mutations (CGTGGC, TGTGGC, AGTGGC, GCTGGC, GATGGC, GTTGGC, GGTGAC, and GGTTGC, where the underlined bases are the sites of the mutations; open and hatched circles in Fig. 1) were used for hybridization.

A mixture of 5′-fluorescein isothiocyanate-labeled oligonucleotides complementary to the wild-type (GGTGGC) and mutant (GATGGC, CGTGGC, and AGTGGC) sequences were used as hybridization probes in a standard dilution mixture series. The ratios of wild type to mutant (in μmol/L) in the mixtures were 0:10, 2:8, 4:6, 6:4, 8:2, and 10:0. In addition, mixtures of genomic DNA prepared from cell lines were amplified and then subjected to the microarray analysis.

Before hybridization, the test site of each array was washed with 1 mL/L Tween 20 for one pumping cycle. Amplification products (108 bp) were generated with 5′-fluorescein isothiocyanate-labeled primers, denatured for 3 min at 94 °C, and cooled to 4 °C on ice. The target DNA, which was 10 μL of either denatured PCR product or oligonucleotide mixture, was mixed with 40 μL of 1.25× standard saline phosphate–EDTA in the well of a PamChip microarray preheated to 55 °C, and the hybridization was started immediately in the FD10 system. In this flow-through hybridization analysis, the liquid flow

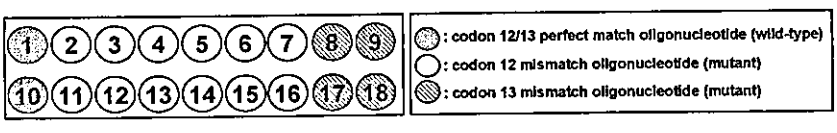

Fig. 1. PamChip microarray layout.

Wild-type (*shaded circles*) and/or mutant (*open* and *hatched circles*) probes were used for hybridization. *Numbers* correspond to those in Table 1 of the online Data Supplement (available at http://www.clinchem.org/content/vol50/issue8/).

rate was 10 μL/s. After 30 cycles (~10 min) of flow-through hybridization at 55 °C, each array was washed once with 1× standard saline phosphate–EDTA with pumping. Array images were captured automatically on the FD10 system and then analyzed with the integrated image acquisition and analysis software.

Results

To examine assay reproducibility and accuracy, we used three PamChip microarrays, each of which contained four test channels. Mixtures of oligonucleotides complementary to wild-type and mutant-type probes were hybridized to the PamChip microarray in duplicate. Signal intensities were not always consistent with the theoretical mixture ratio, however, because there were dose–response effects in each mixture. Representative results obtained with the different ratios of the mixture of GGTGGC (wild type) and GATGGC (mutant) are shown in Fig. 2A. In addition, we used mixtures of genomic DNA prepared from cell lines in the different ratios. Representative results obtained with the mixture of MKN45 (wild-type; GGTGGC) and Lu65 (mutant; TGTGGC) are shown in Fig. 2B.

We tested both sense and antisense strands as hybridization probes. In general, the sense strand identified genotypes more accurately. Results of the PamChip microarray analysis of a homozygous wild-type specimen (GGTGGC) with sense and antisense oligonucleotides as hybridization probes are shown in Fig. 3. A single strong signal for GGTGGC was observed when the sense strand was used as a probe, whereas weak, noisy signals were observed with the antisense probes. We therefore used the sense strand probe in further analyses.

Wild-type, heterozygous, and homozygous mutant genotypes were detected accurately and reliably in 15 cell lines with the PamChip microarray in a relatively short

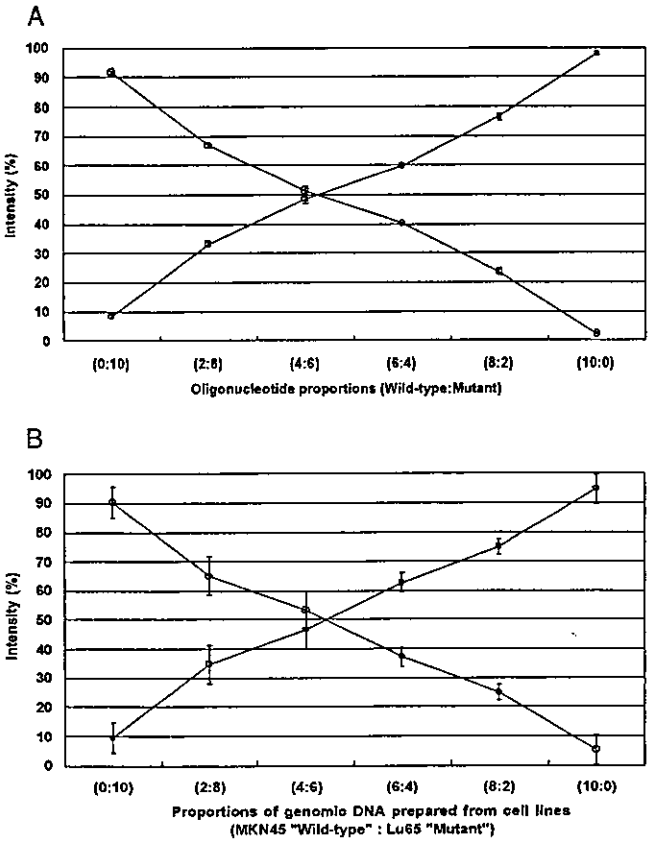

Fig. 2. Fluorescence intensities obtained with complementary oligonucleotides (*A*) and genomic DNA (*B*).

(*A*), relationship between hybridization signal intensity and oligonucleotide population ratio. The fluorescence intensities of hybridization signals were examined with use of the complementary oligonucleotides GGTGGC and GATGGC. The relative fluorescence intensities in mixtures consisting of GGTGGC (□) and GATGGC (○) were calculated by the following formulas: GGTGGC (%) = GGTGGC signal intensity/(GGTGGC signal intensity + GATGGC signal intensity) × 100; and GATGGC (%) = GATGGC signal intensity/(GGTGGC signal intensity + GATGGC signal intensity) × 100. (*B*), representative results obtained with the mixture of genomic DNA prepared from two cell lines, MKN45 (wild-type; GGTGGC) and Lu65 (mutant; TGTGGC). The fluorescence intensities were calculated as described above. □, wild-type intensities; ○ mutant intensities. Each *symbol* represents the mean of four independent microarray results (*error bars*, SD).

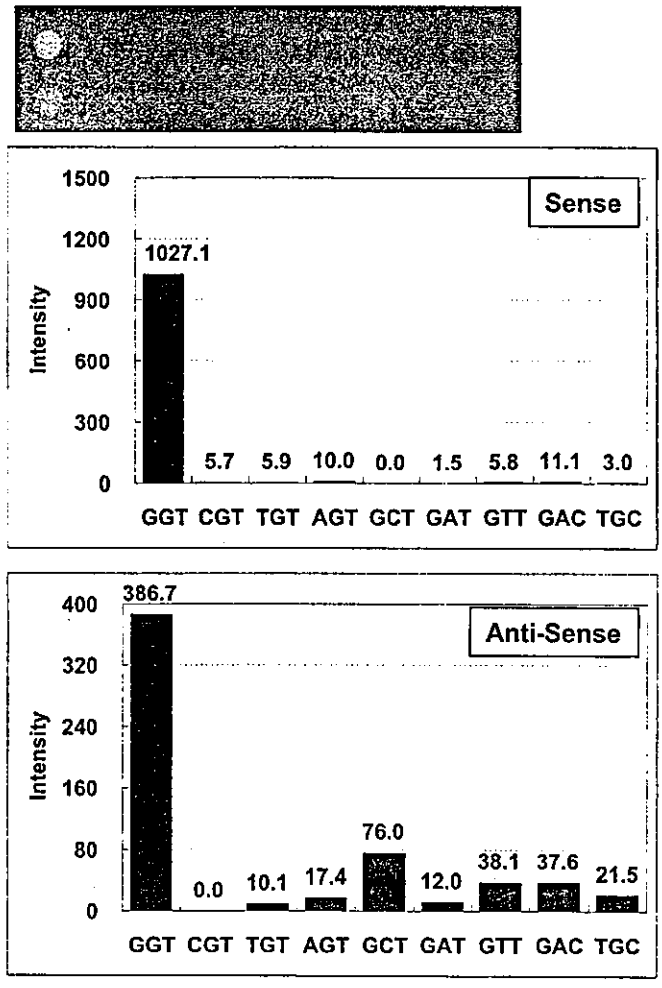

Fig. 3. Comparison of sense and antisense strands as hybridization probes.

Hybridization images in the *top* and *bottom rows* in the *array* (*top*) represent the results obtained with the sense and antisense strands, respectively, used as hybridization probes. The subsequent data analyses (*middle* and *bottom*) show the comparison quantitatively.

time. All results correlated with those of PCR-SSCP analysis and DNA sequencing. DNAs from clinical specimens were also analyzed with the PamChip microarray for comparison with PCR-SSCP analysis and/or DNA sequencing. Fig. 4 shows examples of images captured on the FD10 system and results of subsequent data analyses. Essentially, the results obtained with the PamChip microarray were consistent with those of PCR-SSCP analysis and DNA sequencing. Eighty-one clinical cancer specimens were analyzed with the PamChip microarrays, and the genotypes of 80 of these specimens (98.8%) were identified accurately. PCR-SSCP analysis detected all 64 samples homozygous or heterozygous for mutant genotypes in codon 12. The remaining 17 (of 81) specimens were homozygous or heterozygous for mutant alleles in codon 13, but they could not be identified by SSCP analysis because mutant alleles in codon 13 were not used as a reference for SSCP. Although SSCP bands in 12 of the 17 samples were clearly different from those of the wild-type alleles, the remaining 5 samples were misclassified into the mutant genotype, GATGGC, because of the similar electrophoretic pattern. Therefore, the distinct misidentification was 5, and genotyping succeeded in 76 of 81 samples (93.8%). Thirty-six samples (10 homozygous and 26 heterozygous mutant genotypes) were analyzed by direct DNA sequencing. The 10 samples homozygous for mutant genotypes were identified properly. Twenty-two of the 26 heterozygous mutant samples were misclassified into homozygous wild type, and only the remaining 4 samples were correctly identified. In total, 14 of 36 samples (38.9%) were diagnosed accurately.

Only one sample, a clinical specimen from a patient with colorectal cancer, was classified incorrectly by the PamChip microarray. PamChip analysis yielded a homozygous wild-type genotype, whereas SSCP analysis and DNA sequencing indicated that the genotype was GGTGGC/GATGGC. The semiquantitative proportions obtained by densitometric analysis of SSCP bands were then compared with PamChip microarray and direct DNA sequencing data. The results for clinical specimens are shown in Table 2 of the online Data Supplement. The samples were heterozygous for wild-type and mutant alleles in various proportions. In the single misdiagnosed clinical specimen, the content of the mutant allele was

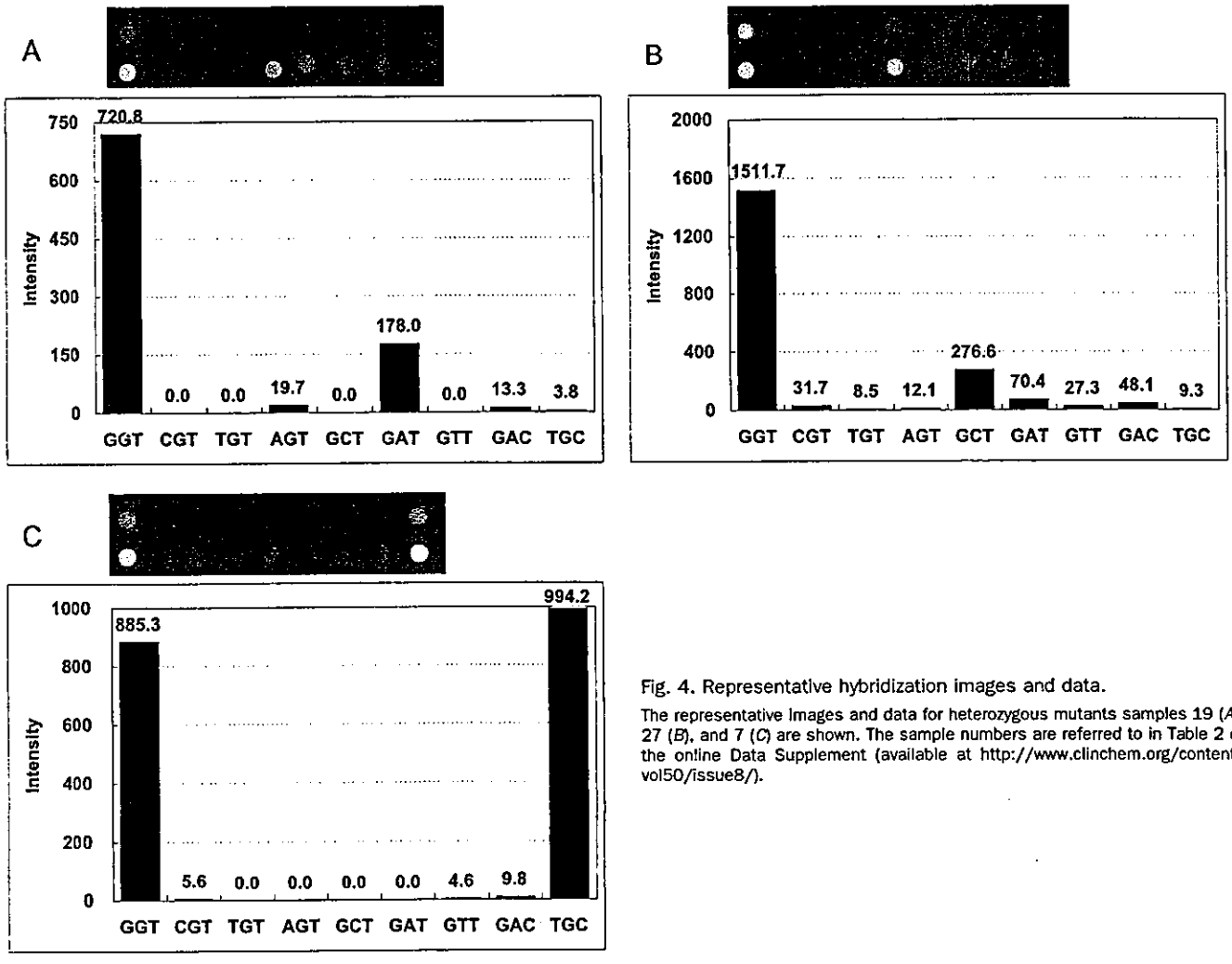

Fig. 4. Representative hybridization images and data.

The representative images and data for heterozygous mutants samples 19 (*A*), 27 (*B*), and 7 (*C*) are shown. The sample numbers are referred to in Table 2 of the online Data Supplement (available at http://www.clinchem.org/content/vol50/issue8/).